Families of Homeomorphic Subsets of the Mandelbrot Set

Wolf Jung
Inst. f. Reine u. Angew. Mathematik, RWTH Aachen
Templergraben 55, D-52062 Aachen, Germany
http://www.iram.rwth-aachen.de/~jung
jung@iram.rwth-aachen.de

Version as of June 22, 1999.

Abstract

The 1/3-limb of the Mandelbrot set $\mathcal{M}$ is considered as a graph, where the vertices are given by certain Misiurewicz points. The edges are described as a union of building blocks that are called "frames". There is a 1–1 correspondence between these frames and star-shaped subsets of the Julia set $\mathcal{K}_a$, where a denotes the Misiurewicz point $\gamma_M(11/56)$. This global combinatorial correspondence between $\mathcal{M}_{1/3}$ and $\mathcal{K}_a$ provides a complement to the asymptotic similarity obtained by Tan Lei.

The frames are defined by recursions for external angles or para-puzzles. By quasi-conformal surgery we construct a homeomorphism h of the edge from a to $\gamma_M(23/112)$ onto itself, and show that the frames on this edge are homeomorphic. This can be generalized to all edges of $\mathcal{M}_{1/3}$, and to all limbs of $\mathcal{M}$. The method is similar to that of Branner–Douady and Branner–Fagella, but the construction of the "first return map" is different.

This paper is available from http://www.ma.utexas.edu/mp_arc/ as 99-???.ps. The latest version is obtained from the author's home page as jg-99-2.ps.

The reader is encouraged to obtain the program **mandel.exe** from the author's home page. This DOS-program draws the Mandelbrot set and Julia sets with a number of different algorithms, finds centers and Misiurewicz points. External rays can be drawn in the dynamical- and the parameter plane. A demo explains the usage and applications of the program.
(The images in the appendix have been made with this program.)

1 Introduction

The Mandelbrot set $\mathcal{M}$ contains those parameters $c \in \mathbb{C}$, such that the filled Julia set $\mathcal{K}_c$ of $f_c(z) = z^2 + c$ is connected. See Section 2 for some basic properties and standard notations that are used in this section. The principal Misiurewicz point of the limb $\mathcal{M}_{1/3}$ is $a := \gamma_M(11/56)$, it satisfies $f_a^3(a) = \alpha_a$. The Julia set $\mathcal{K}_a$ of $z^2 + a$ is a branched curve: locally connected, with empty interior. Tan Lei [19] has shown that both $\mathcal{M}$ at $c \approx a$ and $\mathcal{K}_a$ at $z \approx a$ are asymptotically self-similar and similar to each other, see Section 8. These sets are sketched in the left part of Figure 1.

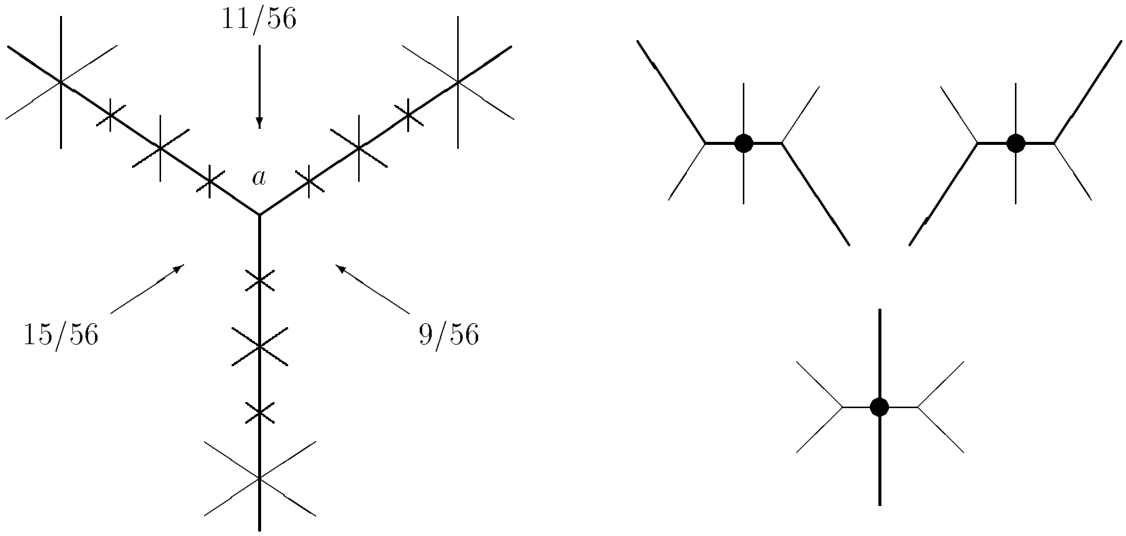

Figure 1: Left: Magnification of $\mathcal{M}$ around $c \approx a$ or $\mathcal{K}_a$ around $z \approx a$, with $a = \gamma_M(11/56)$. Right: Typical subsets of $\mathcal{M}_{1/3}$ on the three arcs incident to a, corresponding to six-stars in $\mathcal{K}_a$. The upper ones are "parameter frames".

The arcs of $\mathcal{K}_a$ are filled with six-stars, that are preimages of the three-star at $z = a$. Close to $c = a$, $\mathcal{M}$ contains subsets that look similar to six-stars. Each of these contains a distinguished tuned copy $\mathcal{M}_0$ of $\mathcal{M}$, and the four arms of the six-star are attached to $\mathcal{M}_0$ in different ways on the three arcs at a, cf. the right part of Figure 1. The whole arc from $a = \gamma_M(11/56)$ to $\gamma_M(23/112)$ is filled with subsets of this form, which will be called "parameter frames". The largest frame is the part of $\mathcal{M}$ between the Misiurewicz points $\gamma_M(177/896)$ and $\gamma_M(183/896)$, it contains the period-4 component at $\gamma_M(3/15)$. This paper has a combinatorial and a surgical part: In the first part, we describe $\mathcal{M}_{1/3}$ as a graph, and the edges are decomposed into frames. In the second part, we use quasi-conformal surgery to construct a homeomorphism, which maps frames onto frames.

1.1 The edges of $\mathcal{M}_{1/3}$

The limb $\mathcal{M}_{1/3}$ is described as an infinite graph, with three edges at every vertex. The vertices are certain Misiurewicz points, and the edges are subsets of $\mathcal{M}_{1/3}$, connecting two vertices. This graph can be defined and motivated in several ways:

- For $c \in \mathcal{M}_{1/3}$, the preimages of α_c have in general three external angles. Some of these undergo a bifurcation as c varies in $\mathcal{M}_{1/3}$, and some have the same external angles for all $c \in \mathcal{M}_{1/3}$. The latter form the vertices of $\mathcal{K}_c$ (considered as a graph). As c varies, the shape of the edges is changing, but the structure of the graph remains the same. The graph of $\mathcal{M}_{1/3}$ is defined by means of the graph of $\mathcal{K}_c$, it has the same external angles at its vertices. This approach is explained in detail in Sections 3 and 4.

- We give a short introduction to para-puzzles in Section 5. In general the subdivision of (para-)puzzle-pieces into finer pieces is possible in different ways. If we only subdivide the sector-shaped pieces and keep the strip-shaped pieces, we arrive at the graph: Each strip contains a unique edge.

- The vertices can also be defined by recursions for external angles, and by the following property: Suppose that b is a vertex of order n, thus $f_b^n(b) = \alpha_b$. Now $\mathcal{M}_{1/3}\backslash\{b\}$ has three connected components, and the one pointing outward to the left contains a unique Misiurewicz point b' with $f_{b'}^{n+1}(b') = \alpha_{b'}$. This characterizes the next vertex b', and defines the edge from b to b'. Similarly, the component pointing to the right contains a unique vertex b'' of order $n+2$. Thus the vertices (and their external angles) are obtained recursively.

An edge of $\mathcal{M}_{1/3}$ contains a topological arc joining the vertices (by a Theorem of Schleicher [18]). $\mathcal{M}_{1/3}$ equals the graph plus an exceptional set, which is a Cantor set.

1.2 Dynamical frames

The three connected components of $\mathcal{M}_{1/3} \setminus \{a\}$ are labeled "trunk" and "left/right upper branch". For c in the upper branches or $c = a$, the edges of $\mathcal{K}_a$ are decomposed into a family of dynamical frames $\mathcal{F}_n^c(u,\, v)$ plus an exceptional set, see Section 6. The frames are defined by the external angles of certain points, which satisfy some recursion, and the family has a hierarchical structure. (The angles are given in terms of the parameters $n,\, u,\, v \in \mathbb{N}$.)

- An edge of $\mathcal{K}_a$ contains a unique arc joining the vertices. The arcs are filled with six-stars, and the vertices of these stars are dense in the arc. The four arms of a six-star define a dynamical frame $\mathcal{F}_n^a(u,\, v)$. The six external angles of the vertex are obtained recursively, and the recursion defines a hierarchy: If the "largest" frame in the "middle" of the arc has the order $n = n_0$, then there are two frames of the order $n = n_0 + 3$, four of order $n = n_0 + 6$, ..., see Figure 6 on page 18. This is explained by the fact that the arc from α_a to $-\alpha_a$ is mapped 2–1 onto itself by f_a^3. The vertex is mapped to a by f_a^n and to α_a by f_a^{n+3}.

- For c in the upper branches of $\mathcal{M}_{1/3}$, a dynamical frame $\mathcal{F}_n^c(u,\, v)$ has the same six characteristic external angles as $\mathcal{F}_n^a(u,\, v)$, but these belong to two different points. The frame has a similar structure as the sets in the right part of Figure 1. The partition of six angles into two groups of three, and thus the pattern of the arms, is uniform in the two branches of $\mathcal{M}_{1/3}$. For c in the left branch, the first arm is pointing to the right and the second arm to the left. f_c maps $\mathcal{F}_n^c(u,\, v) \to \mathcal{F}_{n-1}^c(u',\, v')$, unless the frame contains 0.

- Consider the strip-shaped puzzle-piece corresponding to an edge of $\mathcal{K}_c$, it is subdivided into five pieces in the way of the bottom left or right of Figure 4 on page 13. The three parts in the middle define the largest frame, and if the two outer strips are subdivided in the same way, the two frames on the next level of the hierarchy are obtained. As for the graph, we have a rule that says which puzzle-pieces shall be subdivided and which are not.

The decomposition of $\mathcal{K}_c$ into edges and frames is uniform in the left branch of $\mathcal{M}_{1/3}$ in the following sense: The frames have the same characteristic external angles, and they are mapped onto each other in the same way. As c varies in $\mathcal{M}_{1/3}$, only the shape of the frames is changing.

1.3 Parameter frames

We describe the parameter frames for the left and the right branch of $\mathcal{M}_{1/3}$, but there are no frames on the trunk. A parameter frame is marked by six external rays landing at two Misiurewicz points, and the external angles are the same as for the corresponding dynamical frame, see Section 7. They satisfy the same recursion, and every edge contains a hierarchy of frames plus an exceptional set, which is presumably a Cantor set. $\mathcal{F}_n^M(u,\, v)$ is contained in three para-puzzle-pieces of depth $n+3$, and these are obtained recursively in the same way as for the dynamical frames. The most important property of the parameter frames is that all frames on the same edge are homeomorphic, see below. Now we shall describe some results on the combinatorial level:

- A parameter frame $\mathcal{F}_n^M(u,\, v)$ contains a hyperbolic component Ω_0 of period n, and no other component of a period $\le n+3$. Denote by $\mathcal{M}_0$ the tuned copy of $\mathcal{M}$ with the main cardioid Ω_0.
- The frame $\mathcal{F}_n^M(u,\, v)$ corresponds to the six-star $\mathcal{F}_n^a(u,\, v)$ both by the equality of characteristic external angles, and by Tan Lei's asymptotic similarity. Two arms of the six-star correspond to the arms of the parameter frame, uniformly in the left branch, cf. Figure 1. The other two arms correspond to the middle part of the frame, and some of their tips correspond to the antennas attached to the Ω_0-tuned copies of $\mathcal{M}_{1/3}$ and $\mathcal{M}_{2/3}$.
- The similarity of Tan Lei provides a correspondence between parameter frames and dynamical frames close to a, at most on the incident edges (and there is a different correspondence at any other vertex). On a qualitative level, we

obtain a global correspondence between the regions $9/56 \leq \arg_M(c) \leq 15/56$ in $\mathcal{M}$ and $9/56 \leq \arg_a(z) \leq 15/56$ in $\mathcal{K}_a$.

- According to [10] there is a sequence of centers c_n with periods $n = 4, 7, 10, \ldots$ approaching a on the left edge, see Section 8. We show that each c_n is the center of the Ω_0 for some "six-star" $\mathcal{F}_n^M(u_n, v_n)$. This was observed in [15, p.248] (without a proof). The sequence $\{c_n\}$ is generalized to a hierarchy: One center of period 4, two of period 7, four of period 10, ...

- In Section 9 we show that parameter frames on the same edge contain additional arms which reflect the position of the edge in the graph. We describe hierarchies on subsets of a frame and the structure of some critical orbits.

The notions and properties of edges and frames generalize to all limbs of $\mathcal{M}$. This is announced in Section 10, and we give some formulas for $\mathcal{M}_{1/2}$. In real interval dynamics, the interval corresponding to the tuned copy $\mathcal{M}_0$ is called a "window", since it is visible as a window in the bifurcation diagram. The name "frame" is motivated by the fact that every parameter frame in $\mathcal{M}_{1/2}$ contains a distinguished window. To classify all hyperbolic intervals, it is sufficient to classify all windows that are not contained within another window. The hierarchies of frames are a step towards such a classification, since every frame contains some of these primitive windows. The hierarchies of frames on different limbs will be compatible with the homeomorphisms of Branner–Douady [1] and Branner–Fagella [4].

1.4 Quasi-conformal surgery

See Section 11 for an introduction to quasi-conformal surgery and to the method of [1, 4]. Our surgical procedure is outlined in Section 12. The technique is similar to that of Branner–Douady and Branner–Fagella. The main differences are:

- We do not construct a Riemann surface by adding pieces to or removing pieces from the dynamical plane, but stay in $\mathbb{C}$.

- Our construction of the "first return map" g is different, since we cannot set $g = f^n$ on some pieces. On an edge of $\mathcal{K}_c$ some parts are stretched and others are shrinked, by functions of the form $g = f^{-n} \circ (\pm f^m)$.

For c in the parameter edge $\mathcal{E}_M$ from $a = \gamma_M(11/56)$ to $\gamma_M(23/112)$ we construct a quasi-regular mapping by deforming the critical edge from $\gamma_c(11/56)$ to $\gamma_c(23/112)$ in three pieces. g_c is not holomorphic in some sectors, but we find a g_c-invariant ellipse field and a holomorphic function equivalent to g_c. The Straightening Theorem [8] yields a hybrid equivalence to a polynomial f_d with $d \in \mathcal{E}_M$, and $h : \mathcal{E}_M \to \mathcal{E}_M$ is defined by $h(c) = d$. Now h is a homeomorphism which maps frames onto frames. In fact, all parameter frames in $\mathcal{E}_M$ are homeomorphic. h is analytic in the interior of $\mathcal{E}_M$ and compatible with tuning.

The details of the construction of h are given in Section 13, and we prove in Sections 14 and 15 that h is a homeomorphism. $h(c)$ can be computed practically from the induced mapping of external angles, see Section 16. Some generalizations are discussed in Section 17: Similar homeomorphisms can be constructed on all edges of all limbs, and these will be compatible with Branner–Douady's $\Phi_A : \mathcal{M}_{1/2} \to \mathcal{M}_{1/3}$ and Branner–Fagella's $\Phi^q_{pp'} : \mathcal{M}_{p/q} \to \mathcal{M}_{p'/q}$.

In [14] we show that certain polynomial curves join centers of different periods. Again, these combinatorial relations are compatible with Φ_A. The p-curves form a cobweb around $c = a$, and there is an analogous cobweb around $z = a$ in the dynamical plane for f_a. These cobwebs correspond to each other by Tan Lei's similarity.

2 Preliminaries

Every quadratic polynomial can be conjugated by an affine mapping to $f_c(z) = z^2 + c$ for a unique parameter $c \in \mathbb{C}$. The *Mandelbrot set* $\mathcal{M}$ contains those parameters $c \in \mathbb{C}$ for which the *Julia set* $\mathcal{J}_c$ of f_c is connected, or equivalently, for which the orbit of the *critical point* 0 (or the *critical value* c) is bounded (by 2). $\mathcal{J}_c$ is the boundary of the *filled-in Julia set* $\mathcal{K}_c$, which contains those $z \in \mathbb{C}$ with bounded orbit. Nice introductions are [2, 5, 6].

Suppose that f_b has an attracting n-cycle, thus $f_b^n(z_0) = z_0$ with n minimal, and the *multiplier* $\lambda = (f_b^n)'(z_0)$ satisfies $|\lambda| < 1$. Then the critical value b is attracted to the cycle [5], in particular we have $b \in \mathcal{M}$ and there is no other attracting cycle. b belongs to a *hyperbolic component* $\Omega = \Omega_b$ of the interior of $\mathcal{M}$, and for every $c \in \Omega$, f_c has an attracting n-cycle, and the corresponding multiplier $\lambda = \rho(c)$ maps Ω conformally onto the unit disk $\mathbb{D}$ [5]. $\rho^{-1}(\lambda)$ has a continuous extension to the boundary, and $c = \gamma_\Omega(t)$ is defined by $\rho(c) = \mathrm{e}^{i2\pi t}$. It has the *internal argument* $0 \le t < 1$, which is measured in full turns. The *center* c_0 of the component satisfies $\rho(c_0) = 0$, 0 and c_0 belong to a superattracting cycle of f_{c_0}. The *root* $c_r = \gamma_\Omega(0)$ satisfies $\rho(c_r) = 1$. If $t = k/m$ (in lowest terms), then $\gamma_\Omega(t)$ is the root of a hyperbolic component with period $m \cdot n$, that forms a satellite of Ω. Ω is called a *primitive component*, if its root is not on the boundary of another hyperbolic component. In this case, Ω is cardioid-shaped. Denote the main cardioid by Ω_0. The *limb* $\mathcal{M}_{k/m}$ is connected with Ω_0 at $\gamma_{\Omega_0}(k/m)$. The fixed points of f_c are $\alpha_c = 1/2 - \sqrt{1/4 - c}$ and $\beta_c = 1/2 + \sqrt{1/4 - c}$. For $c \in \Omega_0$, α_c is attracting.

For sufficiently large $|z|$, the mapping

$$\Phi_c(z) = z \prod_{n=1}^{\infty} \Big(1 + \frac{c}{(f_c^{n-1}(z))^2}\Big)^{1/2^n} \tag{1}$$

is well defined, where the roots are understood as principal values. The functional equation $\Phi_c(f_c(z)) = (\Phi_c(z))^2$ shows that Φ_c conjugates $z^2 + c$ to z^2 in a neighborhood of infinity and is used for an analytic continuation of Φ_c. If the orbit of 0 is bounded, then Φ_c maps the exterior of $\mathcal{K}_c$ conformally onto the exterior of the closed unit disk, and in particular, $\mathcal{J}_c$ and $\mathcal{K}_c$ are connected. If the critical orbit is unbounded, then the unique continuation breaks down at a figure-8 curve, and one shows that $\mathcal{K}_c = \mathcal{J}_c$ is a Cantor set [5]. But for $c \notin \mathcal{M}$, $\Phi_M(c) := \Phi_c(c)$ is well defined. Douady and Hubbard have shown that Φ_M maps $\mathbb{C} \setminus \mathcal{M}$ conformally onto the exterior of the closed unit disk, and in particular, the Mandelbrot set $\mathcal{M}$ is connected [5]. Famous conjectures are that $\mathcal{M}$ is locally connected (MLC), and that every component of the interior of $\mathcal{M}$ is hyperbolic. The first would imply the second.

The *external argument* θ with $0 \le \theta \le 1$ is defined by $2\pi \arg_c(z) := \arg(\Phi_c(z))$ and $2\pi \arg_M(c) := \arg(\Phi_M(c))$. An *external ray* $\mathcal{R}_M(\theta)$ in the parameter plane or, for fixed $c \in \mathcal{M}$, a ray $\mathcal{R}_c(\theta)$ in the corresponding dynamical plane, is the curve defined by $\arg_M(c) = \theta$ or $\arg_c(z) = \theta$, respectively. At least for rational values of θ, the ray terminates at a point denoted by $c = \gamma_M(\theta) \in \partial\mathcal{M}$ or $z = \gamma_c(\theta) \in \mathcal{J}_c$, which is said to have the *external angle* θ. In the dynamical plane, the dynamics of $\gamma_c(\theta)$ under f_c reflect those of θ under doubling (modulo 1), since $f_c(\gamma_c(\theta)) = \gamma_c(2\theta)$. The fixed point β_c has the external angle 0, and α_c has m external angles for $c \in \mathcal{M}_{k/m}$. In the parameter plane, the root of a period-n hyperbolic component has two external angles $\theta_\pm = \frac{u_\pm}{2^n-1}$, which have a n-periodic dyadic expansion (for $n = 1$, the angle $0 = 1$ is counted twice). The corresponding *wake* is bounded by $\mathcal{R}_M(\theta_-)$ and $\mathcal{R}_M(\theta_+)$. There is a partial ordering for the hyperbolic components, where $\Omega \prec \Omega'$, iff Ω' is in the wake of Ω. Lavaurs' algorithm allows to determine the qualitative location of hyperbolic components from the pairing of their external arguments [6]. A *Misiurewicz point* $b \in \mathcal{M}$, for which the critical value b is preperiodic under f_b, is the landing point of some external rays with preperiodic angle (i.e. θ has even denominator) [5, 17]. In the dynamical plane, $b \in \mathcal{K}_b$ has the same external angles. Both $\mathcal{M}$ at $c \approx b$ and $\mathcal{K}_b$ at $z \approx b$ are asymptotically self-similar and similar to each other [19].

Suppose that Ω is a hyperbolic component of period n. According to [8] and [9], there is a homeomorphism of $\mathcal{M}$ onto a subset of $\mathcal{M}$, the Ω-*tuned* copy of $\mathcal{M}$, such that the main cardioid is mapped onto Ω, and a period-p component is mapped onto a component of period $n \cdot p$. The induced mapping of external arguments is described in [6] and [7]: Denote by $\theta_\pm = \frac{u_\pm}{2^n-1}$ the external angles of (the root of) Ω and consider the integers $u_\pm$ as binary numbers with n digits (thus $\theta_\pm = .\overline{u_\pm}$). An angle θ landing at $\mathcal{M}$ is tuned by replacing the digit 0 in its binary expansion by u_- and 1 by u_+. Example: We have $1/2 = .0\bar{1} = .1\bar{0}$, and the Misiurewicz point $-2 = \gamma_M(1/2)$ is tuned by Ω to a Misiurewicz point b with the external angles $.u_-\overline{u_+}$ and $.u_+\overline{u_-}$. Between these rays, another part of $\mathcal{M}$ is attached to the tuned copy, and there may be further external rays landing at b. In real dynamics, the interval between b and the root of Ω is called a *window*. If Ω is attached to the main cardioid Ω_0 at $\gamma_{\Omega_0}(k/m)$, we shall say that b is the *principal* Misiurewicz point of the limb $\mathcal{M}_{k/m}$. It satisfies $f_b^m(b) = \alpha_b$ and has m external angles, that are preimages (under doubling) of the external angles of α_c.

Part I: Combinatorics

3 Basic Dynamics for c in the 1/3-Limb of $\mathcal{M}$

Denote the main cardioid by Ω_0 and the period-3 component in the upper halfplane by $\Omega_{1/3}$. The root of $\Omega_{1/3}$ is $c_r = \gamma_{\Omega_0}(1/3)$, and its external angles are given by $\theta_-(\Omega_{1/3}) = 1/7 = .\overline{001}$ and $\theta_+(\Omega_{1/3}) = 2/7 = .\overline{010}$. The 1/3-wake lies between the external rays $\mathcal{R}_M(1/7)$ and $\mathcal{R}_M(2/7)$, and the corresponding part of the Mandelbrot set is the 1/3-limb $\mathcal{M}_{1/3}$. (An equivalent definition of the limb relies on the fact that $\mathcal{M} \setminus \{c_r\}$ has two connected components. The upper one union with $\{c_r\}$ yields $\mathcal{M}_{1/3}$.)

For $c \in \mathcal{M}_{1/3}$, the fixed point α_c of f_c has the external angles 1/7, 2/7 and 4/7, and $\mathcal{K}_c \setminus \{\alpha_c\}$ has three connected components. A typical $\mathcal{K}_c$ is shown in the left part of Figure 2 on page 10. The six external rays landing at $\pm\alpha_c$ divide the dynamical plane into five parts. f_c maps $12 \to 20$, $20 \to 01 \cup 02 \cup 00$, $02 \to 20$ and $00 \to 01 \cup 02 \cup 00$ bijectively, and $01 \to 12$ as a double covering. The notation for these parts as puzzle-pieces of depth 1 is explained in Section 5. The preimages of $01 \cup 02 \cup 00$ have a natural subdivision into three parts, and a further division is obtained recursively. The preimages of α_c and their external angles are important to describe the structure of $\mathcal{K}_c$. We define $A_0^c = \{\alpha_c\}$ and for $n \in I\!N$

$$A_n^c = \left\{z \,\middle|\, f_c^n(z) = \alpha_c\,,\ f_c^{n-1}(z) \neq \alpha_c\right\} = \left\{z \,\middle|\, f_c^{n-1}(z) = -\alpha_c\right\} \qquad (2)$$

$$C_n^c = \left\{z \,\middle|\, f_c^n(z) = c\right\}. \qquad (3)$$

The following Lemma gives some elementary properties of these sets:

Lemma 1 *Consider f_c with $c \in \mathcal{M}_{1/3}$.*

1. *We have $z \in A_n^c$, iff z has an external angle θ with*

$$\theta = \frac{k}{7 \cdot 2^n}\,,\ k \equiv 1\,,\ k \equiv 9 \text{ or } k \equiv 11 \ (\mathrm{mod}\, 14)\,. \qquad (4)$$

2. *If $f_c^l(c) \neq \alpha_c$ for all $l \in I\!N$, then each $z \in A_n^c$ has three external angles, and we have $|A_n^c| = 2^{n-1}$.*

3. *If $f_c^l(c) = \alpha_c$ and $f_c^{l-1}(c) \neq \alpha_c$ (thus c is a special Misiurewicz point), then we have $C_j^c \subset A_{j+l}^c$. Now $z \in C_j^c$ has six external angles, and $z \in A_n^c \setminus C_{n-l}^c$ has three external angles.*

4. *$|C_j^c| = 2^{j-1}$, if c is not the center of a hyperbolic component of $\mathcal{M}$.*

5. *The Misiurewicz point a with $f_a^3(a) = \alpha_a$ has the external angles 9/56, 11/56 and 15/56. We have $z \in C_n^a$, iff z has an external angle θ with*

$$\theta = \frac{k}{7 \cdot 2^{n+3}}\,,\ \ k \equiv 9\,,\ k \equiv 11 \text{ or } k \equiv 15 \ (\mathrm{mod}\, 56)\,. \qquad (5)$$

Proof of Lemma 1:
1.: $f_c^{n-1}(z) = -\alpha_c$ has the external angles 1/14, 9/14 and 11/14, and $2^{n-1}\theta$ is one of these.
2.: f_c is locally injective except at the critical point 0. Here 0 is not a preimage of α_c, thus f_c^n is locally injective at $z \in A_n^c$.
3.: c has three external angles, and its only preimage 0 has six external angles, since f_c is $2-1$ in a neighborhood of 0.
4.: We have $C_1^c = \{0\}$ and $f_c^{j-1}(z) = 0$ for $z \in C_j^c$. Since $f_c^k(z) \neq 0$ for $0 \le k \le j-2$, f_c^{j-1} is locally injective at z.
5.: The principal Misiurewicz point a of $\mathcal{M}_{1/3}$ satisfies $f_a^3(a) = \alpha_a$. $9/56 = .001\overline{010}$ and $15/56 = .010\overline{001}$ are obtained by tuning $1/2 = .0\bar{1} = .1\bar{0}$. 11/56 is obtained from $a \in A_3^a$ and (4). For (5), compare the proof of (4). ∎

Suppose that $b \in \mathcal{M}_{1/3}$ and $z_* \in A_n^b$ are such that $f_b^j(z_*) \neq b$ for $1 \le j \le n-3$. This condition will be met, if b satisfies $f_b^l(b) \neq \alpha_b$ for $3 \le l \le n-1$. Then there is a neighborhood U of b and a function $z = z_c$ depending analytically on $c \in U$ with $z_b = z_*$, such that $z_c \in A_n^c$ and z_c has the same three external angles for $c \in U$. To show this, note that f_b^n is locally injective at z_*. Thus we have $z_c = (f_c^n)^{-1}(\alpha_c)$ for a suitable branch of $(f_c^n)^{-1}$, which depends analytically on $c \in U$.

Now suppose that $b \in \mathcal{M}_{1/3}$ with $f_b^l(b) = \alpha_b$ for a $l \ge 3$. For any $n \ge l+1$ and $z_* \in A_n^b \cap C_{n-l}^b$, a bifurcation takes place at z_* for $c = b$: The three external rays landing at b bound three sectors in the parameter plane, and in a neighborhood U of b intersected with a sector, there are analytic functions z_c and z_c' with $z_c \in A_n^c$ and $z_c' \in A_n^c$, and these points have the same three external angles each. For $c \to b$, both $z_c \to z_*$ and $z_c' \to z_*$, and z_* has six external angles. The partition of six angles into two groups of three is different in the three connected components of $\mathcal{M}_{1/3} \setminus \{b\}$ (intersected with U). This fact motivates the definition of para-puzzles, cf. Section 5: The rays landing at b separate some para-puzzle-pieces of depth l.

The simplest example is provided for $l = 3$ and $n = 4$: Consider the Misiurewicz point a with $f_a^3(a) = \alpha_a$ and the external angles 9/56, 11/56 and 15/56. Then there are $z_c, z_c' \in A_4^c$ which coincide with 0 for $c = a$. Their six external angles 9/112, 11/112, 15/112, 65/112, 67/112 and 71/112 are combined in different ways in the three connected components of $\mathcal{M}_{1/3} \setminus \{a\}$, as illustrated in the lower part of Figure 4 on page 13. For $c = a$, all six rays terminate at 0.

4 Graphs

For $n \in I\!N$, denote by Σ_n the set of external angles θ satisfying (4), and such that for all j with $1 \le j \le n-3$ we have $2^j\theta \notin (1/7,\, 2/7) \pmod 1$. For $c \in \mathcal{M}_{1/3}$, define $V_n^c := \{\gamma_c(\theta) \,|\, \theta \in \Sigma_n\} \subset A_n^c$. (Equivalently: V_n^c contains those $z \in A_n^c$, such that no iterate $f_c^j(z)$, $j \in I\!N$, lies between the external rays with the angles 1/7 and 2/7.) Moreover, set $\Sigma_0 = \{1/7,\, 2/7,\, 4/7\}$ and $V_0^c = \{\alpha_c\}$. According to the statements at the end of Section 3, $\gamma_c(\theta)$ has the same three external angles for $c \in \mathcal{M}_{1/3}$, if

$\theta \in \Sigma_n^c$, and its external angles undergo a bifurcation, if θ satisfies (4) but $\theta \notin \Sigma_n^c$. Denote by c_0 the period-3 center in $\mathcal{M}_{1/3}$. The "Douady rabbit" is the filled-in Julia set $\mathcal{K}_{c_0}$ of f_{c_0}, it is sketched in the left part of Figure 2. The interior of $\mathcal{K}_{c_0}$ consists of a countable family of simply connected components. Ω_0 shall be the component containing 0. The vertices of Ω_0 shall be $\pm\alpha_{c_0}$, and the sides of Ω_0 contain hierarchies of preimages of α_{c_0}: Two points in $A_4^{c_0}$, four in $A_7^{c_0}$, eight in $A_{10}^{c_0}$ .... To every vertex, two components are attached, and we obtain a graph with three edges at every vertex. These vertices are precisely the points in $\bigcup\limits_n V_n^c$: They are never mapped to the region 12, and if $z_* \in A_n^{c_0}$ is attached (indirectly) to a side of a component, it will be mapped to a side of Ω_0, and these are mapped into the region 12 between the rays for 1/7 and 2/7.

Figure 2: The Douady rabbit and the graph of $\mathcal{K}_c$ for $c \in \mathcal{M}_{1/3}$, cf. Lemma 2.

Lemma 2 *We construct a graph by means of the sets V_n^c defined at the beginning of this section:*

1. *For $c \in \mathcal{M}_{1/3}$, the graph of $\mathcal{K}_c$ is defined as follows: The vertices are $\bigcup\limits_n V_n^c$, and the connected components of $\mathcal{K}_c \setminus \bigcup\limits_n V_n^c$ are called edges. Every edge is incident to two vertices, and they form an infinite, simply connected graph with three edges at every vertex. The abstract graphs are isomorphic for all $c \in \mathcal{M}_{1/3}$, with the same three external angles at corresponding vertices. See Figure 2.*

2. *For $\theta \in \Sigma_n$ with $1/7 < \theta < 2/7$, $b = \gamma_M(\theta)$ is a Misiurewicz point with $f_b^n(b) = \alpha_b$. It has the same three external angles as $\gamma_c(\theta) \in \mathcal{K}_c$ for all $c \in \mathcal{M}_{1/3}$. Denote by V_n^M the set of these points b, and $V_0^M = \{\gamma_M(1/7)\}$. The graph of $\mathcal{M}_{1/3}$ is constructed analogously to paragraph 1. It is a subgraph of the graph of $\mathcal{K}_c$, cf. Figure 3.*

3. *The external arguments $\bigcup\limits_n \Sigma_n$ of the graph of $\mathcal{K}_c$ for $c \in \mathcal{M}_{1/3}$ are determined recursively as follows: Suppose that $z' \in V_n^c$ and $z'' \in V_m^c$ are adjacent vertices with z' closer to α_c than z'' (counting edges), thus $n < m$. Their external*

angles shall be denoted as it is sketched in the upper right part of Figure 4 on page 13. Then we have

$$\theta_1 = \phi + \frac{1}{8}(\psi - \phi) \qquad \theta_2 = \phi + \frac{3}{8}(\psi - \phi) \qquad \theta_3 = \phi + \frac{7}{8}(\psi - \phi) \tag{6}$$

(with $0 < \psi - \phi < 1$). The same relations hold for the graph of $\mathcal{M}_{1/3}$.

Presumably, 1. and 2. are well-known but not published explicitly, and 3. is elementary. If $\mathcal{K}_c$ is locally connected, every edge contains a topological arc joining the vertices. If a point in an edge has external angles on both sides of the edge, it will lie on the arc. By Theorem 5.6 in [18], the edges of $\mathcal{M}_{1/3}$ contain topological arcs. Both $\mathcal{K}_c$ and $\mathcal{M}_{1/3}$ consist of the graph plus an exceptional set. Each exceptional point corresponds to an infinite sequence of edges approaching it, and every such sequence corresponds to a single point by the method of divergence [3, 12, 16].

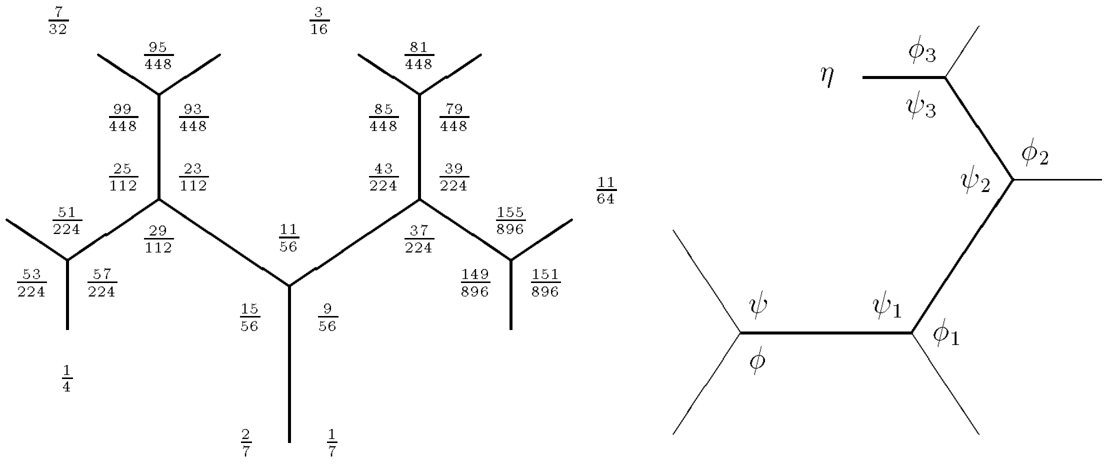

Figure 3: Left: The graph of $\mathcal{M}_{1/3}$ with some external angles, cf. Lemma 2. Right: Recursions, cf. (8).

Proof of Lemma 2: 1. The graph of $\mathcal{K}_{c_0}$ was constructed above. Since the external angles of $z_c \in V_n^c$ do not undergo a bifurcation, it can be constructed in the same way for all $c \in \mathcal{M}_{1/3}$, and only the shape of the edges depends on c.
2. Here $b \in \mathcal{M}_{1/3}$ has the same three external angles as $b \in \mathcal{K}_b$, and these are the same for $\gamma_c(\theta)$ with $c \in \mathcal{M}_{1/3}$, since $\theta \in \Sigma_n$. There is a unique graph joining the vertices of $\mathcal{M}_{1/3}$ without intersecting an external ray $\mathcal{R}_M(\tilde{\theta})$ for $\tilde{\theta} \in \bigcup_m \Sigma_m$, since the corresponding part of the graph of $\mathcal{K}_c$ is determined uniquely.
3. We have $f_c^{m-1}(z') = \alpha_c$ and $f_c^{m-1}(z'') = -\alpha_c$. The statement follows from the external angles of these two points. More precisely, there is a $w \in \mathbb{Z}$, such that

$$\phi = \frac{14w + 8}{7 \cdot 2^m} \qquad \psi = \frac{14w + 16}{7 \cdot 2^m} \qquad \text{and} \tag{7}$$

$$\theta_1 = \frac{14w + 9}{7 \cdot 2^m} \qquad \theta_2 = \frac{14w + 11}{7 \cdot 2^m} \qquad \theta_3 = \frac{14w + 15}{7 \cdot 2^m} \; . \qquad \blacksquare$$

The number of vertices of order n forms a Fibonacci sequence:

$$|V_1^c| = 1\,,\ |V_2^c| = 2\,,\ |V_3^c| = 4\,,\quad |V_n^c| = |V_{n-1}^c| + |V_{n-2}^c| \quad \text{for} \quad n \ge 4$$

$$|V_3^M| = 1\,,\ |V_4^M| = 1\,,\quad |V_n^M| = |V_{n-1}^M| + |V_{n-2}^M| \quad \text{for} \quad n \ge 5\ .$$

Consider multiple turns left, as sketched in the right part of Figure 3. Then the equation (6) yields a linear recursion, and we obtain

$$\phi_m \;=\; \frac{(2^m+3)\phi + 3(2^m-1)\psi}{2^{m+2}} \qquad \psi_m \;=\; \frac{(2^m-1)\phi + (3\cdot 2^m+1)\psi}{2^{m+2}}\ . \tag{8}$$

Both ϕ_m and ψ_m tend to $\eta = \dfrac{\phi + 3\psi}{4}$ for $m \to \infty$. The denominator of η is the least possible power of 2 for angles between ϕ and ψ.

5 Puzzles and Para-Puzzles

Before describing the (modified) Yoccoz-puzzle, we shall present a general but vague concept of symbolic dynamics. Suppose that $c \in \mathcal{M}$ and Γ_0^c is the union of some curves in the dynamical plane, often such that $f_c(\Gamma_0^c) \subset \Gamma_0^c$, and $\mathbb{C} \setminus \Gamma_0^c$ or $(\mathbb{C} \setminus \mathcal{K}_c) \setminus \Gamma_0^c$ consists of a finite number of connected parts $A_1^c, \ldots, A_N^c$. To z we associate a sequence of symbols $(s_0^c, s_1^c, s_2^c, \ldots)(z)$ such that $s_n^c(z) = A_j$, if $f_c^n(z) \in A_j^c$, and $s_n^c(z) = *$, if $f_c^n(z) \in \Gamma_0^c$. If z is n-periodic, the sequence $(s_n^c(z))$ will have a period dividing n. For any n, the plane is divided into a finite number of connected pieces, such that $s_0^c(z), \ldots, s_n^c(z)$ are the same for all z in the same piece. To c we associate the sequence $(s_n^c(c))$ and divide the parameter plane accordingly. If Γ_0^c consists of rational dynamical rays, the pieces in the parameter plane will be bounded by rational parameter rays.

The simplest example is the following: For $c \in \mathcal{M}$, Γ_0^c consists of the rays $\mathcal{R}_c(0)$ and $\mathcal{R}_c(1/2)$. The exterior of $\mathcal{K}_c$ is divided into two parts. If the upper one is called 0 and the lower one is called 1, the resulting symbol sequence is just the binary expansion of the external argument of z, and $(s_n^c(c))$ yields the external argument of $c \in \mathbb{C} \setminus \mathcal{M}$ (in this case, the definition of dynamical rays is more involved). See Section 16 for an application. It is not customary to consider pieces for this partition, but they would be separated by rays $\mathcal{R}_*(k/2^{n+1})$.

As another example, suppose that $c = \gamma_M(\theta)$ (or c belongs to a hyperbolic component with its root at $\gamma_M(\theta)$). Now Γ_0^c consists of $\mathcal{R}_c(\frac{\theta}{2})$ and $\mathcal{R}_c(\frac{1+\theta}{2})$ (and some curve joining their endpoints), and $\mathbb{C} \setminus \Gamma_0^c$ consists of two parts L and R, with $c \in L$. The symbol sequence $(s_n^c(z))$ is called the *itinerary* of z, and $(s_n^c(c))$ is the *kneading sequence* of c (if c has several external angles, all yield the same sequence). For $c \in \mathbb{R}$, we have $s_n^c(c) = L$, iff $f_c^n(c) < 0$. Thus the kneading sequence of an external angle generalizes the usual concept of real interval dynamics. See [13] for details and applications. We will need itineraries in Section 9.1.

The Yoccoz-puzzle is defined separately for every limb of $\mathcal{M}$. For $c \in \mathcal{M}_{k/m}$, α_c has m external angles, and the corresponding dynamical rays form Γ_0^c. The m

sectors between these rays are labeled 0, 1, ..., $m-1$ according to $f_c^j(0) \in j$. The *puzzle sequence* $(s_n^c(z))$ satisfies the following restriction: If $1 \le s_n^c(z) \le m-2$, then $s_{n+1}^c(z) = s_n^c(z) + 1$, and if $s_n^c(z) = m-1$, than $s_{n+1}^c(z) = 0$. In the case of $s_n^c(z) = 0$, there is no restriction on $s_{n+1}^c(z)$. The *para-puzzle* sequence $(s_n^c(c))$ has the additional property $s_1^c(c) = 1$. The *puzzle-pieces* of depth n are separated by the external rays that are mapped into Γ_0^c by f_c^n. They land at points z with $f_c^n(z) = \alpha_c$, thus $z \in \bigcup_{j=0}^{n} A_j^c$. The *para-puzzle-pieces* are separated by parameter rays with the same angles (in the interval corresponding to $\mathcal{M}_{k/m}$). They land at Misiurewicz points c with $f_c^n(c) = \alpha_c$. For all c in a para-puzzle-piece of depth n, the subdivision of the dynamical plane into puzzle-pieces of depth $n+1$ is (qualitatively) the same. This fact is related to the kind of bifurcation described at the end of Section 3. The puzzle-pieces of depth 1 for $c \in \mathcal{M}_{1/3}$ are shown in the left part of Figure 2 on page 10.

Usually the puzzles and para-puzzles are defined in a different way, such that Γ_0^c contains a level curve of the Green's function, thus the closed pieces are compact. This is not necessary for our application, and we shall use unbounded pieces. Basic references for (para-) puzzles are [3], [12] and [16]: In certain cases one shows that a nested sequence of pieces contains a single point, which implies that a Julia set or the Mandelbrot set at some point is locally connected. See [18] for a generalization of this approach. Para-puzzle-pieces are homeomorphic to certain puzzle-pieces, this is explained in [12, p.499].

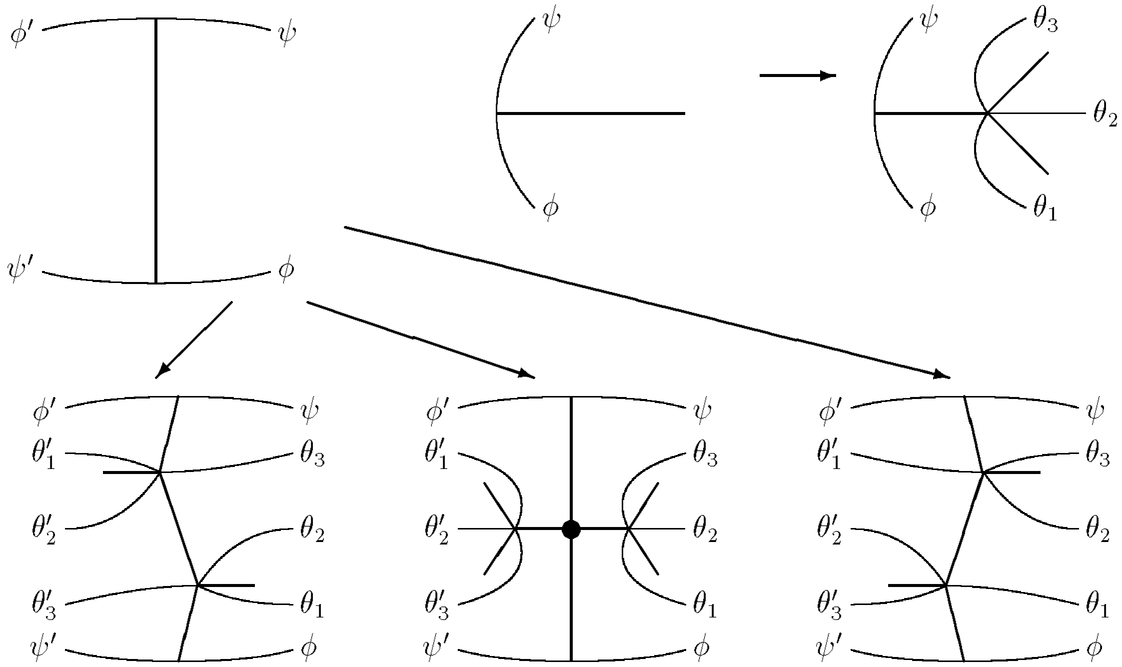

Figure 4: Partition of some puzzle-pieces or para-puzzle-pieces for $c \in \mathcal{M}_{1/3}$. The external angles are related by (6). (The thin lines are external rays, and the thick lines represent subsets of $\mathcal{K}_c$ or $\mathcal{M}_{1/3}$.)

An unbounded piece according to our modified definition may be a sector, bounded by two rays landing at one point, or a strip, bounded by four rays meeting at two points, ore some more involved structure. If $s_n^c(z) = 0$ for z in some puzzle-piece of depth n, then this piece consists of some pieces of depth $n+1$, as it is sketched in Figure 4 for $c \in \mathcal{M}_{1/3}$. The relevant angles satisfy the equation (6). A sector consists of one strip and two sectors. This kind of subdivision corresponds to the construction of the graph in Section 4. A strip is decomposed in one of three possible ways (if c is not a Misiurewicz point). To find the right one, first map the strip onto another one containing 0. This strip is mapped onto a sector containing c. Observing the position of c in the subdivision of this sector, the subdivision of the original strip is obtained. The simplest example was mentioned at the end of Section 3: The strip $01 = 0120$ is subdivided into puzzle-pieces of depth 4 in three different ways for c in the three connected components of $\mathcal{M}_{1/3} \setminus \{a\}$, which correspond to the following para-puzzle-pieces of depth 3: 1200, 1201 and 1202. All pieces of depth 4 are drawn in [3, p.54] and [12, p.483] (or with mandel.exe). Although it is easy to obtain the puzzle-pieces of depth n for small values of n, it is in general not possible to give a description for all n. The family of dynamical frames defined in Lemma 5 will consist of preimages of the first decomposition of 0120, thus it contains special puzzle-pieces of arbitrarily large order. The para-puzzle-pieces of depth n are determined from puzzle-pieces for different values of c, thus it is not straightforward that some of these have the same structure. But the families of parameter frames defined in Theorem 6 correspond to dynamical frames and thus have a similar structure.

6 Dynamical Frames

The dynamical frames are constructed first for the Julia set $\mathcal{J}_a = \mathcal{K}_a$ of $a = \gamma_M(11/56)$. This Misiurewicz point satisfies $f_a^3(a) = \alpha_a$, thus $C_n^a \subset A_{n+3}^a$. The Julia set is a dendrite, in particular, it is locally connected, and every edge of the graph contains a unique topological arc joining the vertices. These arcs are filled with six-stars, as it is sketched in Figure 6 on page 18. These six-stars will be called "frames", and we describe them in terms of hierarchies in Theorem 4. First we give a preparatory Lemma, containing the definition of a frame with some parameters.

Suppose that $\mathcal{A} \subset \mathcal{K}_a$ is a topological arc joining two vertices of the graph of $\mathcal{K}_a$, thus $\mathcal{A}$ corresponds to an edge $\mathcal{E}$. z', $z'' \in \bigcup_m A_m^a$ shall be located on $\mathcal{A}$, with z' "closer" to α_a than z''. ϕ, ψ, ϕ' and ψ' shall be external angles of z' and z'', as it is sketched in Figure 5. If z' or z'' has six external angles, we take those closest to $\mathcal{A}$. It will be useful to assume that there are parameters n, u, $v \in I\!\!N$ with

$$\phi = \frac{7u+1}{7 \cdot 2^n} \qquad \psi = \frac{7u+2}{7 \cdot 2^n} \qquad \phi' = \frac{7v+1}{7 \cdot 2^n} \qquad \psi' = \frac{7v+2}{7 \cdot 2^n} \ . \tag{9}$$

(Some of these fractions are in lowest terms, and some are not.) We are looking for $z \in \bigcup_m A_m^a$ in the part of $\mathcal{E}$ between z' and z'', which is contained in the strip bounded by the four external rays. By (4) we need a θ with $\phi < \theta_i < \psi$, such that the denominator of θ is of the form $7 \cdot 2^m$. Now $\dfrac{14u+3}{7 \cdot 2^{n+1}}$ does not satisfy the congruence relation of (4), thus it does not land at a $z \in A^a_{n+1}$. In the same way we see that $\dfrac{28u+5}{7 \cdot 2^{n+2}}$ and $\dfrac{28u+7}{7 \cdot 2^{n+2}}$ do not land at $z \in A^a_{n+2}$. The same applies to $\phi' < \theta'_i < \psi'$. The six external angles given by

$$\theta_1 = \frac{56u+9}{7 \cdot 2^{n+3}} \qquad \theta_2 = \frac{56u+11}{7 \cdot 2^{n+3}} \qquad \theta_3 = \frac{56u+15}{7 \cdot 2^{n+3}} \tag{10}$$

$$\theta'_1 = \frac{56v+9}{7 \cdot 2^{n+3}} \qquad \theta'_2 = \frac{56v+11}{7 \cdot 2^{n+3}} \qquad \theta'_3 = \frac{56v+15}{7 \cdot 2^{n+3}}$$

satisfy (4) and land at one or two points of A^a_{n+3}. Now $2^n\theta_1 \equiv \frac{9}{56} \pmod 1$ lands at a, thus θ_1 lands at a $z_0 \in C^a_n$, which has six external angles, these must be $\theta_1, \ldots, \theta'_3$. Since the corresponding external rays are on both sides of $\mathcal{A}$, we have $z_0 \in \mathcal{A}$. We define the frame $\mathcal{F}^a_n(u, v)$ to be the union of the four arms of $\mathcal{K}_a$ meeting at z_0. The point z_0 will be called the central vertex, not to be confused with a vertex of the graph. According to the remarks on (8), the rays with the following external angles land at "tips" as sketched in Figure 5:

$$\begin{array}{llll} \eta_1 = \dfrac{16u+3}{2^{n+4}} & \eta_2 = \dfrac{4u+1}{2^{n+2}} & \rho_1 = \dfrac{64u+11}{2^{n+6}} & \rho_2 = \dfrac{32u+7}{2^{n+5}} \\ \eta'_1 = \dfrac{16v+3}{2^{n+4}} & \eta'_2 = \dfrac{4v+1}{2^{n+2}} & \rho'_1 = \dfrac{64v+11}{2^{n+6}} & \rho'_2 = \dfrac{32v+7}{2^{n+5}} \end{array} \tag{11}$$

We have obtained the following

Lemma 3 *Consider z', $z'' \in \bigcup_m A^a_m$ located on an arc $\mathcal{A} \subset \mathcal{K}_a$ corresponding to an edge of the graph, with z' "closer" to α_a than z''. The external angles of z' and z'' shall be ϕ, ψ, ϕ' and ψ' as it is sketched in Figure 5. Suppose that there are $n, u, v \in \mathbb{N}$ with (9). Then*

1. *No $z \in A^a_1 \cup A^a_2 \cup \ldots \cup A^a_{n+2}$ lies in the strip bounded by the four external rays.*

2. *There is exactly one $z_0 \in A^a_{n+3}$ in this strip. It satisfies $z_0 \in C^a_n$ and belongs to the arc $\mathcal{A}$.*

3. *The six external angles of z_0 are given by (10). Note that this is equivalent to the recursion (6).*

The frame $\mathcal{F}^a_n(u, v)$ is the connected subset of $\mathcal{K}_a$ that consists of $\{z_0\}$ and the four "smaller" arms at z_0 (thus $\mathcal{R}_a(\theta)$ lands at $\mathcal{F}^a_n(u, v)$, iff $\theta_1 \le \theta \le \theta_3$ or $\theta'_1 \le \theta \le \theta'_3$).

Now suppose that $n_0 \in \mathbb{N}$ and $\mathcal{A}$ is an arc of the graph of $\mathcal{K}_a$, joining $z' \in A^a_{n_1}$ and $z'' \in A^a_{n_0}$ with $n_1 < n_0$. By (7), the angles ϕ, ψ, ϕ', ψ of Figure 5 can be written (modulo 1) as

$$\phi = \frac{14w+8}{7 \cdot 2^{n_0}} \qquad \psi = \frac{14w+9}{7 \cdot 2^{n_0}} \qquad \phi' = \frac{14w+15}{7 \cdot 2^{n_0}} \qquad \psi' = \frac{14w+16}{7 \cdot 2^{n_0}} .$$

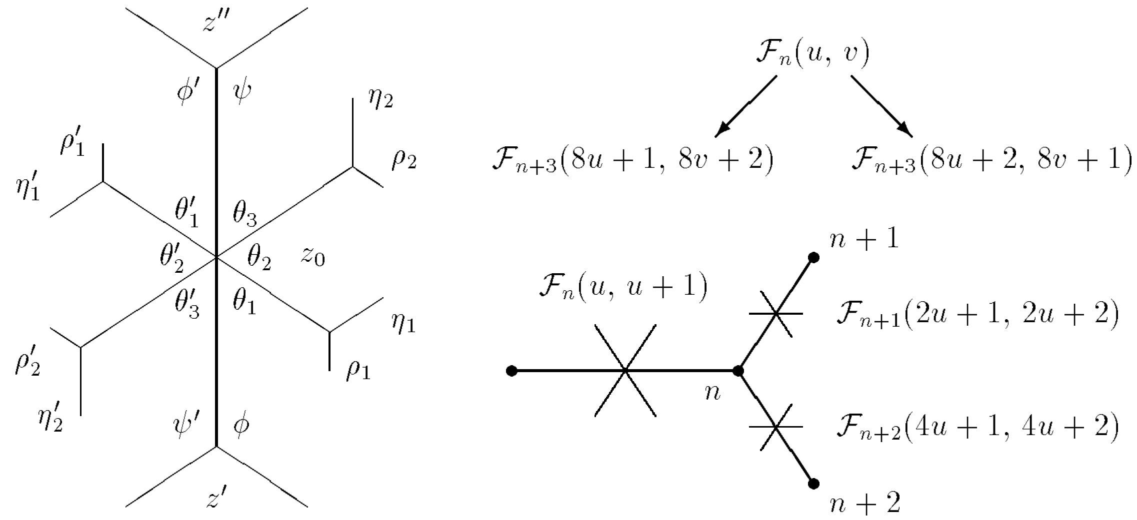

Figure 5: Left: A frame $\mathcal{F}_n^a(u,\, v)$ for $\mathcal{K}_a$, $a = \gamma_M(9/56)$, cf. Lemma 3. Right: Recursions, cf. Theorem 4.

Thus (9) is satisfied with $n = n_0$, $u = u_0 = 2w+1$ and $v = v_0 = u_0 + 1 \pmod{2^{n_0}}$. By Lemma 3, $\mathcal{F}_{n_0}^a(u_0,\, v_0)$ is the largest frame on $\mathcal{A}$. We shall now show that there are two frames with $n = n_0 + 3$ on $\mathcal{A}$. This is the first step of a recursion which yields a hierarchy of frames, an example is sketched in Figure 6. Denote the central vertex of $\mathcal{F}_{n_0}^a(u_0,\, v_0)$ by z_0. The half arc from z' to z_0 has the bounding external angles $\tilde\phi = \phi$, $\tilde\psi = \theta_1$, $\tilde\phi' = \theta'_3$ and $\tilde\psi' = \psi'$, and we can apply Lemma 3 again with the new parameters $\tilde n = n_0 + 3$, $\tilde u = 8u_0 + 1$ and $\tilde v = 8v_0 + 2$. The half arc contains the frame $\mathcal{F}_{n_0+3}^a(8u_0+1,\, 8v_0+2)$. Its central vertex belongs to $C_{n_0+3}^a$, and the "half" edge in the strip $\tilde\phi < \arg_a(z) < \tilde\psi$, $\tilde\phi' < \arg_a(z) < \tilde\psi'$ does not contain a $z \in A_m^a$ with $m \le n_0 + 5$. In the same way, we obtain the frame $\mathcal{F}_{n_0+3}^a(8u_0+2,\, 8v_0+1)$ on the half arc from z_0 to z''. Working inductively, we find four frames with $n = n_0 + 6$, eight frames with $n = n_0 + 9\,\ldots$, and this family has a hierarchical structure. This is explained by considering the arc from α_a to $-\alpha_a$: each of its two half arcs is mapped onto the whole arc by f_a^3, cf. Section 9.1.

The recursive application of Lemma 3 shows that the only preimages of α_a on the arc $\mathcal{A}$ are the central vertices of the frames, and that $\{\theta \in [\phi,\, \psi] \,|\, \gamma_a(\theta) \in \mathcal{A}\}$ is some kind of a Cantor set. It is mapped onto $\mathcal{A}$ by some kind of a devil's staircase.

The parameters of all frames on $\mathcal{A}$ are obtained recursively from n_0 and u_0. There is another recursion for the arcs, that is obtained in a similar way from (6): If the largest frame on $\mathcal{A}$ has the parameters $n = n_0$, $u = u_0$ and $v = u_0 + 1$, the arc turning left has $n = n_0 + 1$ and $u = 2u_0 + 1$, and the arc turning right has $n = n_0 + 2$ and $u = 4u_0 + 1$. The recursion starts with the parameters for the arcs incident to α_a. Their largest frames are $\mathcal{F}_1^a(1,\, 0) = \mathcal{F}_1^a(1,\, 2)$, $\mathcal{F}_2^a(1,\, 2)$ and $\mathcal{F}_3^a(1,\, 2)$.

We collect these results in the following

Theorem 4 *Suppose that $n_0 \in I\!N$ and that z', z'' are two adjacent vertices of the graph of $\mathcal{K}_a$ joined by an arc $\mathcal{A}$, with $z'' \in V_{n_0}^a$ and $z' \in V_{n_0-1}^a \cup V_{n_0-2}^a$ or $z' = \alpha_a$.*

1. *Then there are* $u_0,\, v_0 \in I\!N$ *such that the hypotheses of Lemma 3 are satisfied, thus* $\mathcal{A}$ *contains the frame* $\mathcal{F}^a_{n_0}(u_0,\, v_0)$. *Moreover,* $v_0 = u_0 + 1$ *for this frame (or* $v_0 = u_0 + 1 - 2^{n_0}$*).*

2. $\mathcal{A} \setminus \mathcal{F}^a_{n_0}(u_0,\, v_0)$ *contains exactly two frames of order* $n_0 + 3$*:*

   $$z' \prec \mathcal{F}^a_{n_0+3}(8u_0+1,\, 8v_0+2) \prec \mathcal{F}^a_{n_0}(u_0,\, v_0) \prec \mathcal{F}^a_{n_0+3}(8u_0+2,\, 8v_0+1) \prec z'' \,. \tag{12}$$

   From this recursion, an infinite hierarchy of frames with order $\equiv n_0 \pmod 3$ *is obtained inductively, cf. Figure 5 and the example in Figure 6.*

3. *These frames fill out* $\mathcal{A}$ *in the following sense: The angles* θ*, for which* $\mathcal{R}_a(\theta)$ *is landing at* $\mathcal{A}$*, form a set of measure* 0*. The only preimages of* α_a *on* $\mathcal{A}$ *are the central vertices of the frames, in particular, these are preimages of* a *(with six external angles): One point in* C_{n_0}*, two in* C_{n_0+3}*, four in* C_{n_0+6} $\dots$.

4. *There is a simple recursion for the arcs of the graph: The parameters of the "largest" frame are obtained from*

   $$\begin{aligned} \mathcal{F}^a_{n_0}(u_0,\, u_0+1) &\xrightarrow{\text{left}} \mathcal{F}^a_{n_0+1}(2u_0+1,\, 2u_0+2) \\ \mathcal{F}^a_{n_0}(u_0,\, u_0+1) &\xrightarrow{\text{right}} \mathcal{F}^a_{n_0+2}(4u_0+1,\, 4u_0+2)\ , \end{aligned} \tag{13}$$

   cf. Figure 5. Together with the recursion (12), all hierarchies of frames on the graph are obtained.

For every frame on the arc $\mathcal{A}$, the sum of angles $\theta_1 + \theta_3' = \theta_3 + \theta_1'$ is the same and equals $\phi + \psi' = \psi + \phi'$. Now, every arm of a frame is branched to an infinite family of arcs, which in turn contain a family of six-stars ..., but we shall reserve the term "frame" for the six-stars that have their vertex on an arc of the graph. These will be generalized to frames $\mathcal{F}^c_n(u,\, v)$ of $\mathcal{K}_c$ with $c \in \mathcal{M}_{1/3}$ below, and we define a correspondence to subsets $\mathcal{F}^M_n(u,\, v)$ of $\mathcal{M}_{1/3}$ in Section 7.

Lemma 5 *We construct dynamical frames for* c *in the upper branches of* $\mathcal{M}_{1/3}$*:*

1. *Suppose the parameters* $n,\, u,\, v$ *are such that* $\mathcal{F}^a_n(u,\, v)$ *is a frame of* $\mathcal{K}_a$*, and define* $\theta_i,\, \theta_i'$ *by (10). If* c *is in the "left branch" of* $\mathcal{M}_{1/3}$ *(corresponding to the region* $11/56 < \arg_M(c) < 15/56$*), then the six rays* $\mathcal{R}_c(\theta_i)$ *and* $\mathcal{R}_c(\theta_i')$ *land at two points of* A^c_{n+3}*, in the way sketched in the lower left part of Figure 4 on page 13.* $\mathcal{K}_c$ *is sketched in Figure 11 on page 28. If* c *is in the right branch of* $\mathcal{M}_{1/3}$ *(*$9/56 < \arg_M(c) < 11/56$*), then the landing pattern is given by the lower right part of Figure 4.*

2. *In both cases, the dynamical frame* $\mathcal{F}^c_n(u,\, v)$ *shall be the subset of* $\mathcal{K}_c$ *in the strip bounded by the rays for* $\theta_1,\, \theta_3,\, \theta_1'$ *and* θ_3'*. These frames satisfy the recursions (12) and (13), and fill out the edges of* $\mathcal{K}_c$ *(neglecting an exceptional set).*

3. *Every frame is mapped 1–1 onto another one, except for* $\mathcal{F}^c_1(1,\, 0)$*, which is mapped 2–1 onto the region* $9/56 \le \arg_c(z) \le 15/56$*.*

4. We have $0 \in \mathcal{F}_1^c(1,\,0) = f_c^{n-1}(\mathcal{F}_n^c(u,\,v))$*, and* $0 \notin f_c^m(\mathcal{F}_n^c(u,\,v))$ *for* $1 \le m \le n-2$*.*

Presumably, the exceptional set will be a Cantor set (this is not true for $c = a$).

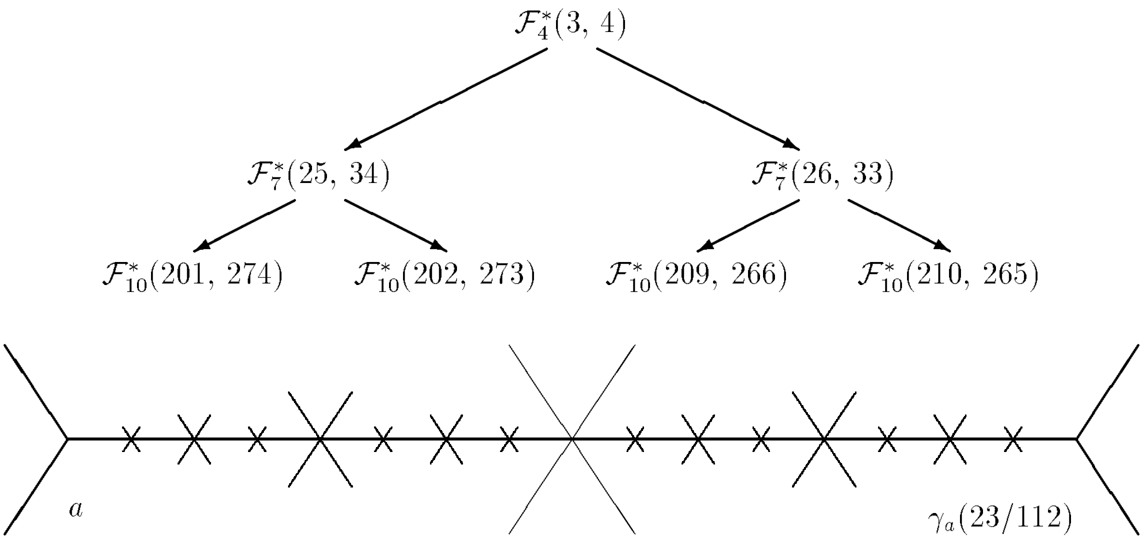

Figure 6: A hierarchy of frames on the arc from a to $\gamma_a(23/112)$ in $\mathcal{K}_a$, cf. Theorem 4, and on the arc from a to $\gamma_M(23/112)$ in $\mathcal{M}_{1/3}$, cf. Theorem 6. (Note that the image is rotated.)

Proof of Lemma 5 (for c in the left branch):
1, 2, 3.: Let us first consider the frame $\mathcal{F}_1^c(0,1)$. The six angles θ_i and θ_i' are preimages of $9/56$, $11/56$ and $15/56$, they land at two points $z_1,\,z_2 \in A_4^c$. By the remarks at the end of Section 3, the landing pattern is the same for all c in the left branch. Now the part of $\mathcal{K}_c$ between α_c and 0 is mapped 1–1 onto the part between α_c and c, in a sense that can be made precise for $c = \gamma_M(\theta)$ with θ rational. The preimage of the arm between (the rays for) $9/56$ and $11/56$ is an arm between $9/112$ and $11/112$, thus these two rays land at the same point z_1, and $15/112$ lands at z_2. For $n > 1$ we have $f_a^{n-1}(F_n^a(u,\,v)) = F_1^a(0,\,1)$. One shows inductively, that the characteristic rays of $\mathcal{F}_n^c(u,\,v)$ land in the same pattern, and thus define a strip (this would not be true for c in the "trunk" of $\mathcal{M}_{1/3}$).
4. For $1 \le m \le n-2$, $f_c^m(\mathcal{F}_n^c(u,\,v)) = \mathcal{F}_{n-m}^c(u',\,v'))$ is a frame of $\mathcal{K}_c$, and $0 \in \mathcal{F}_1^c(1,\,0) \ne \mathcal{F}_{n-m}^c(u',\,v'))$. These frames are disjoint, since the corresponding external angles belong to disjoint intervals, which is obvious from $\mathcal{K}_a$. ■
Now $\mathcal{F}_n^c(u,\,v)$ consists of three puzzle-pieces of depth $n+3$. The partition of $\mathcal{K}_c$ into frames does not involve all puzzle-pieces of a given order, but some pieces of all orders. These belong to the preimages of the pieces of depth 4 in $\mathcal{F}_1^c(1,\,0)$.

7 Parameter Frames in the Mandelbrot Set

Suppose that $\mathcal{F}_n^a(u, v)$ is a dynamical frame for $\mathcal{K}_a$ according to Lemma 3 and Theorem 4, located in the region $11/56 < \arg_a(z) < 15/56$, and define the standard angles by (10) and (11). Consider the dynamical frame $\mathcal{F}_n^b(u, v)$ for the Misiurewicz point $b = \gamma_M(\theta_1)$. By Lemma 5, b has the external angles θ_1, θ_2 and θ_3' in the dynamical plane, and thus in the parameter plane. θ_3, θ_1' and θ_2' belong to another Misiurewicz point. We define the *parameter frame* $\mathcal{F}_n^M(u, v)$ as the subset of $\mathcal{M}_{1/3}$ in the strip bounded by the rays for θ_1, θ_3, θ_1' and θ_3'.

Now $\mathcal{F}_4^M(3, 4)$ is the "largest" frame on the edge/arc from $a = \gamma_M(9/56)$ to $\gamma_M(23/112)$. The recursion (13) yields the largest frame on every edge of this "left branch" of the graph of $\mathcal{M}_{1/3}$, and the recursion (12) yields a hierarchy of frames on every edge. Neglecting an exceptional set, these frames fill out the branch. The exceptional set will presumably be a Cantor set. It contains Misiurewicz points like $\gamma_M(199/1008)$, but it does not contain a hyperbolic component. We consider the frames as building blocks of the branch, which provide a 1–1 correspondence between a family of subsets of a branch of $\mathcal{M}_{1/3}$ and of a branch of $\mathcal{K}_a$. This qualitative correspondence is in some sense global on the branch, while the asymptotic similarity of Tan Lei cannot be defined beyond the edges incident at a (and there are different homeomorphisms at other vertices). On the right branch of $\mathcal{M}_{1/3}$, the frames are defined in a similar way. The landing pattern of the standard angles is different, and the largest frame is $\mathcal{F}_5^M(5, 6)$. The "trunk" cannot be described in this way.

It makes sense to consider these frames as building blocks, if they have an interesting uniform structure. In the second part of this paper we will show that all frames on the same edge are homeomorphic. Here we shall show that a parameter frame $\mathcal{F}_n^M(u, v)$ contains a distinguished tuned copy $\mathcal{M}_0$ of $\mathcal{M}$. The center c_0 of its main cardioid has the period n, and there is no other center with a period $\le n + 3$ within the frame: Define $\theta = \frac{u}{2^n-1}$ and $\theta' = \frac{v}{2^n-1}$. In the left branch, we find $\theta_2 < \theta < \theta_3$ and $\theta_2' < \theta' < \theta_3'$, and $\theta_1 < \theta < \theta_2$, $\theta_1' < \theta' < \theta_3$ in the right branch. One shows that θ and θ' are the only angles with denominator $2^n - 1$ that land at the frame. Thus θ and θ' are external angles of a unique hyperbolic component with a period dividing n. By Lemma 5, we have $0 \notin f_{c_0}^m(\mathcal{F}_n^{c_0}(u, v))$ for $m \le n - 2$, thus the period cannot be less than n. Now suppose that $c \in \mathcal{F}_n^M(u, v)$ is a center with $c \ne c_0$. Then $f_c^n(c)$ is in the region $9/56 < \arg_c(z) < 15/56$, and the period of c will be at least $n + 4$. Especially, c_0 belongs to a primitive component.

To show that $\mathcal{M}_0$ is contained in the frame, either note that $\gamma_M(\theta_3)$ cannot belong to $\mathcal{M}_0$, or consider the tuning of external angles by c_0: $1/2 = .0\overline{1} = .1\overline{0}$ becomes $\sigma = .u\overline{v}$ and $\sigma' = .v\overline{u}$, and one shows $\sigma < \theta_3$ and $\theta_2' < \sigma'$ (for the left branch). Similar frames can be defined on all limbs of $\mathcal{M}$. In the case of $\mathcal{M}_{1/2}$, the frames define intervals on the real axis, cf. Section 10. The interval corresponding to $\mathcal{M}_0$ is called a "window" in real dynamics. This motivates the name "frame".

We have obtained the following

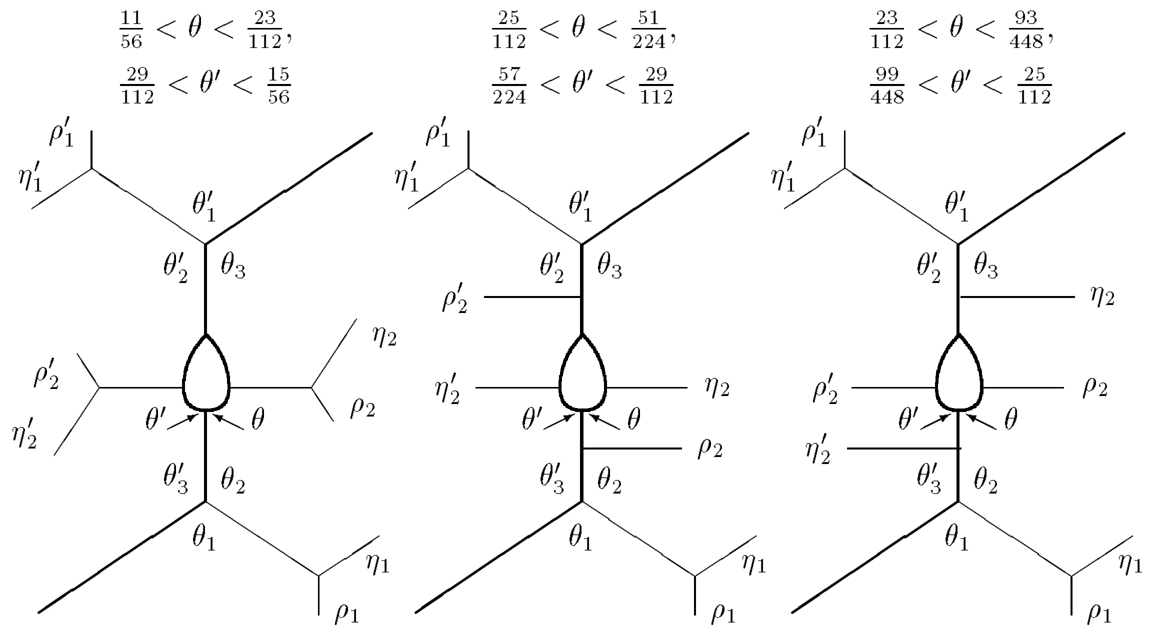

Figure 7: Frames for $\mathcal{M}_{1/3}$ with $11/56 < \theta < 15/56$, cf. Theorem 6 and Lemma 9.

Theorem 6 *The edges of the graph of $\mathcal{M}_{1/3}$ are filled with a hierarchy of frames $\mathcal{F}_n^M(u,\, v)$, which correspond to the frames in $\mathcal{K}_a$. $\mathcal{F}_n^a(u,\, v)$ contains a $z_0 \in C_n^a$, and $\mathcal{F}_n^M(u,\, v)$ contains a hyperbolic component of period n. Thus by external arguments we have a global correspondence between the parts of $\mathcal{M}_{1/3}$ and $\mathcal{K}_a$ bounded by the rays $\mathcal{R}_*(9/56)$ and $\mathcal{R}_*(15/56)$. More specifically,*

1. *For $n,\, u,\, v \in I\!N$ define θ_i, θ_i', η_i, η_i' ρ_i, ρ_i' as in (10), (11). Suppose that the frame $\mathcal{F}_n^a(u,\, v)$ is on an arc of the graph of $\mathcal{K}_a$, with $11/56 < \theta_1$ and $\theta_3' < 15/56$. Then $\mathcal{M}_{1/3}$ contains a frame $\mathcal{F}_n^M(u,\, v)$ as sketched in Figure 7: θ_1, θ_2 and θ_3' land at one Misiurewicz point and θ_3, θ_1' and θ_2' at another one. The frame is the part of $\mathcal{M}_{1/3}$ in the strip between the rays for θ_1, θ_3', θ_3 and θ_1'. The location of η_2, ρ_2, η_2' and ρ_2' varies, see Lemma 9.*

2. *Suppose that the frame $\mathcal{F}_n^a(u,\, v)$ is on an arc of the graph of $\mathcal{K}_a$, with $9/56 < \theta_1$ and $\theta_3' < 11/56$. Then $\mathcal{M}_{1/3}$ contains a frame $\mathcal{F}_n^M(u,\, v)$ as sketched in Figure 8: θ_1, θ_2' and θ_3' land at one Misiurewicz point and θ_2, θ_3 and θ_1' at another one. The frame is the part of $\mathcal{M}_{1/3}$ in the strip between the rays for θ_1, θ_3', θ_3 and θ_1'. The location of η_1, ρ_1, η_1' and ρ_1' varies, see Lemma 9.*

3. *A frame $\mathcal{F}_n^M(u,\, v)$ according to 1. or 2. contains a distinguished tuned copy $\mathcal{M}_0$ of $\mathcal{M}$. Its (primitive) main cardioid has the period n, and there is no other component with a period $\le n+3$ within the frame. The external angles of the root are $\theta = \dfrac{u}{2^n-1}$ and $\theta' = \dfrac{v}{2^n-1}$.*

4. *The hierarchy of frames on an arc satisfies the recursion (12), cf. the example in Figure 6. The recursion (13) yields the "largest" frame on any arc of the graph of $\mathcal{M}_{1/3}$. By Theorem 4, the largest frame $\mathcal{F}_n^M(u,\, v)$ satisfies $v = u+1$.*

Thus the wake of the corresponding period-n component contains no other component with a period $\leq n$.

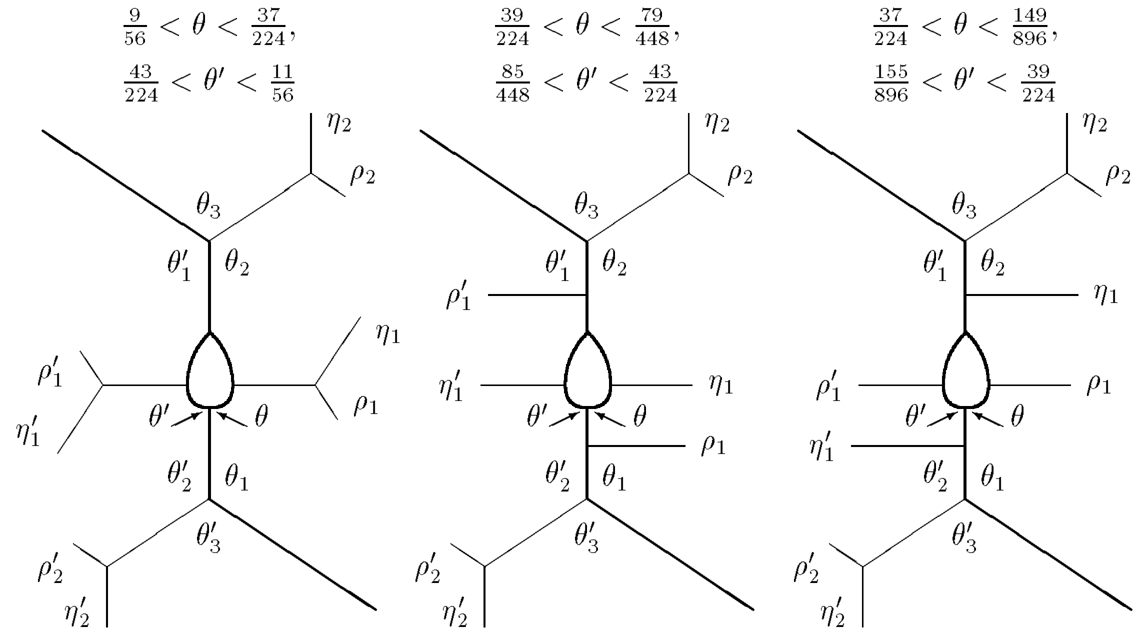

Figure 8: Frames for $\mathcal{M}_{1/3}$ with $9/56 < \theta < 11/56$, cf. Theorem 6 and Lemma 9.

The frames on the two branches are mirror-symmetric to each other both on the combinatorial level, and by the involution of [4]. For the "trunk" between $\gamma_M(1/7)$ and a, some weaker results are obtained in Lemma 7. The parameter frame with the smallest period is $\mathcal{F}_4^M(3,\,4)$. We have $\theta = 3/15$ and $\theta' = 4/15$, the angles θ_i are 177/896, 179/896, 183/896 and the θ_i' are 233/896, 235/896 and 239/896. The frames show a striking combination of symmetries: Most parts of a frame have a (qualitative) rotational symmetry, but $\mathcal{M}_0$ and the other tuned copies of $\mathcal{M}$ on the arc from $\gamma_M(\theta_1)$ to $\gamma_M(\theta_3)$ are symmetric w.r.t. a reflection at this arc. A frame contains many hierarchies of frame-like subsets, see Section 9.2, but these shall not be called "frames".

A frame $\mathcal{F}_n^M(u,\,v)$ consists of three para-puzzle-pieces of depth $n+3$, but we have no combinatorial description for all pieces. An edge in the upper branches of $\mathcal{M}_{1/3}$ corresponds to some strip-shaped piece, and it is subdivided in the way of the lower left or right part of Figure 4 to obtain the largest frame. In the next step of the hierarchy, the two outer strips are divided further in the same way. Only the statements of Lemma 9 correspond to some further subdivision of the inner pieces.

The trunk of $\mathcal{M}_{1/3}$, i.e. the edge from $\gamma_M(1/7)$ to a, cannot be described as a union of parameter frames, because a region corresponding to a dynamical frame $\mathcal{F}_n^a(u,\,v)$ does not form a strip in the parameter plane. We have the following weaker statements:

Lemma 7 *Suppose that the frame $\mathcal{F}_n^a(u,\,v)$ is on the arc from α_a to a, thus* $1/7 < \theta_1 < \theta_3 < 9/56$ *and* $15/56 < \theta_1' < \theta_3' < 2/7$*:*

1. *In the parameter plane, θ_1, θ_2 and θ_3 land at one Misiurewicz point and θ_1', θ_2' and θ_3' land at another one.*
2. *$\theta = \dfrac{u}{2^n - 1}$ and $\theta' = \dfrac{v}{2^n - 1}$ may have a period less than n, and they may land at different roots. Two examples are given in Figure 9.*
3. *By Lemma 8, there is a unique sequence of centers c_3, c_6, c_9, ..., such that c_{n+3} is between c_n and a, and such that c_n has the period n. The external angles are $\dfrac{u_n}{2^n - 1}$ and $\dfrac{v_n}{2^n - 1}$ with $u_n = \frac{9 \cdot 2^{n-3} - 2}{7}$ and $v_n = \frac{15 \cdot 2^{n-3} - 1}{7}$. For these centers, the Misiurewicz points of 1. are attached (not directly) to the $1/3$- and $2/3$-limbs of the c_n-tuned copy of $\mathcal{M}$, as in the left part of Figure 9.*

Proof: 1. For c in the trunk of $\mathcal{M}_{1/3}$, the six dynamical rays for θ_i and θ_i' land in the way sketched in the lower middle part of Figure 4.
2. For $\mathcal{F}_6^a(9, 18)$ we have $\theta = 9/63 = 1/7$. For $\mathcal{F}_9^a(74, 143)$, $\theta = 74/511$ and $\theta' = 143/511$ are external angles of the $1/3$- and $2/3$-satellites of $\Omega_{1/3}$.
3. The external angle of the $\mathcal{M}_{1/3}$-tip is $1/4 = .00\overline{1} = .01\overline{0}$. It is tuned by c_n to $\tau_1 = .u_n u_n \overline{v_n} = \frac{(2^{2n}-1)u_n + v_n}{2^{2n}(2^n-1)}$ and $\tau_2 = .u_n v_n \overline{u_n} = \frac{(2^{2n}-2^n+1)u_n + (2^n-1)v_n}{2^{2n}(2^n-1)}$. Between these angles, a part of $\mathcal{M}$ is attached to the tuned image of the $1/3$-limb. The statement follows from $\tau_1 \le \theta_1 \le \theta_3 \le \tau_2$. ∎

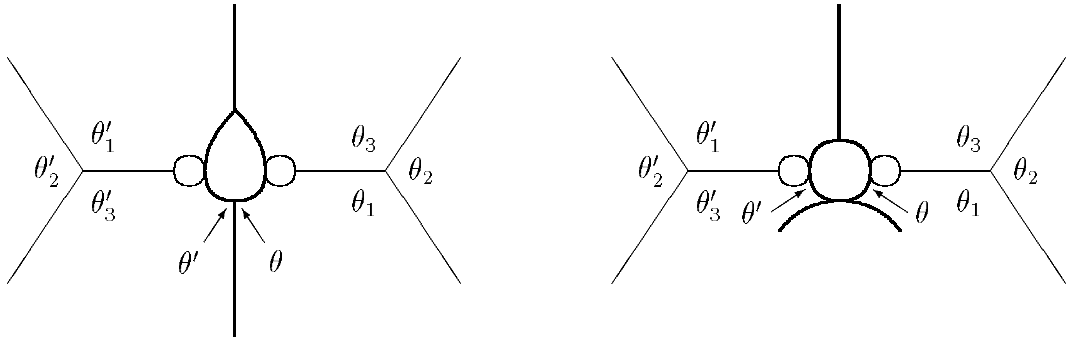

Figure 9: Examples of parameter regions corresponding to dynamical frames $\mathcal{F}_n^a(u, v)$ on the arc from $\alpha_a = \gamma_a(1/7)$ to a, cf. Lemma 7.

8 A Sequence of Centers Spiraling towards a Misiurewicz Point

We shall first describe some results of Tan Lei, Douady–Hubbard and Eckmann–Epstein. Write f_a^{-1} for the inverse of f_a restricted to some neighborhood of α_a, and $\rho_a := f_a'(\alpha_a) = 2\alpha_a$. With respect to the Hausdorff-Chabauty distance of sets, the following limit sets exist [19]:

$$X_a \;:=\; \lim_{k\to\infty} \rho_a^k \, (\mathcal{K}_a - \alpha_a)$$

$$\begin{aligned} Z_a &:= \lim_{k\to\infty} \rho_a^k\,(\mathcal{K}_a - a) \\ Y_a &:= \lim_{k\to\infty} \rho_a^k\,(\mathcal{M} - a)\,. \end{aligned}$$

These asymptotic models are self-similar around 0 with the scale ρ_a. Moreover, with $u(c) := f_c^3(c) - \alpha_c$ we have $Z_a = \dfrac{1}{f_a^{3\prime}(a)} X_a$ and $Y_a = \dfrac{1}{u'(a)} X_a$, thus $Y_a = \lambda\, Z_a$ with $\lambda = \dfrac{f_a^{3\prime}(a)}{u'(a)}$. Similar results hold for every Misiurewicz point. In our case we have

$$\begin{aligned} a &= -.1010963638456 + i\,.9562865108091 \\ \rho_a &= -.6551723573987 + i\,1.1555129065979\,. \end{aligned}$$

The linearizing function $\phi_a(z) := \lim\limits_{k\to\infty} \rho_a^k \left((f_a^{-1})^k(z) - \alpha_a\right)$ satisfies the equation $\phi_a(f_a(z)) = \rho_a\,\phi_a(z)$ for $z \approx \alpha_a$. ϕ_a is a natural homeomorphism $\mathcal{K}_a \to X_a$ around α_a. f_a^3 is injective in a neighborhood of a, and f_a^{-3} shall be the inverse. Then

$$\psi_a(z) := \lim_{k\to\infty} \rho_a^k \left((f_a^{-3} \circ (f_a^{-1})^k \circ f_a^3)(z) - a\right) = \frac{1}{f_a^{3\prime}(a)}\,\phi_a(f_a^3(z))$$

is a natural homeomorphism $\mathcal{K}_a \to Z_a$ around a.

In [10], Eckmann and Epstein showed that there is a sequence of centers c_n with period dividing n, that spirals towards a with $c_n \sim a + K_1\,\rho_a^{-n}$ for some $K_1 \neq 0$. They employ a sequence $\{x_n\}$ spiraling towards α_a, with $f_a^n(x_n) = 0$ and $f_a(x_{n+1}) = x_n$. K_1 is defined by $x_n \sim \alpha_a + u'(a)\,K_1\,\rho_a^{-n-4}$. We define $z_n := f_a^{-3}(x_{n-4})$, then this sequence satisfies $f_a^n(z_n) = a$ and spirals towards a, with $z_n \sim a + \dfrac{K_1}{\lambda}\rho_a^{-n}$. We shall see that z_n is the central vertex of a frame $\mathcal{F}_n^a(u_n,\, v_n)$, and c_n is the distinguished center in $\mathcal{F}_n^M(u_n,\, v_n)$ (at least on two of the three arcs), thus z_n and c_n are related via the external angles of these frames. We have $(z_n - a) \sim \lambda\,(c_n - a)$. Although Tan Lei's result $Y_a = \lambda\,Z_a$ remains true when λ is replaced by $\rho_a^j\,\lambda$, the choice of $j = 0$, which is motivated by the analytical proofs, is also the most natural one regarding the combinatorics of external angles. The proofs in [19] and [10] relate $\mathcal{M}$ at a to $\mathcal{K}_a$ at α_a. Alternatively, one could use the function $F_a := f_a^{-3} \circ f_a \circ f_a^3$ for $z \approx a$, which satisfies $F_a(z_{n+1}) = z_n$. Note that $\psi_a(z) = \lim\limits_{k\to\infty} \rho_a^k \left((F_a^{-1})^k(z) - a\right)$ and $\psi_a(z_n) = \lim\limits_{k\to\infty} \rho_a^k\,(z_{n+k} - a) = \dfrac{K_1}{\lambda}\,\rho_a^{-n}$.

The main result of Eckmann and Epstein is the following: The diameter of the c_n-tuned copy of $\mathcal{M}$ is $\sim K\,\rho_a^{-2n}$. For $n \to \infty$, the arms of the frames have a length $\sim K'\,\rho_a^{-n}$. This explains that the asymptotic model Y_a of $\mathcal{M}$ at a has an empty interior, although the interior of $\mathcal{M}$ is dense in $\mathcal{M}$ [5]. Similar results have been obtained in [8], and we shall give a combinatorial proof of the existence of $\{c_n\}$ below.

Lemma 8 *There is a unique sequence of centers $c_n \in \mathcal{M}_{1/3}$ with period n, $n \geq 3$, spiraling towards a, such that $c_n \to a$ for $n \to \infty$ and c_{n+3} is on the arc from c_n to*

a, and such that c_3, c_4 and c_5 are on different arcs. The external angles of (the root belonging to) c_n are $\dfrac{u_n}{2^n-1}$ and $\dfrac{v_n}{2^n-1}$, where
1. c_3, c_6, c_9, ... are on the arc from $\gamma_M(1/7)$ to a, with $u_n = \frac{9\cdot 2^{n-3}-2}{7}$ and $v_n = \frac{15\cdot 2^{n-3}-1}{7}$.
2. c_4, c_7, c_{10}, ... are on the arc from a to $\gamma_M(23/112)$, with $u_n = \frac{11\cdot 2^{n-3}-1}{7}$ and $v_n = \frac{15\cdot 2^{n-3}-2}{7}$.
3. c_5, c_8 c_{11}, ... are on the arc from a to $\gamma_M(37/224)$, with $u_n = \frac{9\cdot 2^{n-3}-1}{7}$ and $v_n = \frac{11\cdot 2^{n-3}-2}{7}$.
In $\mathcal{K}_a$, there is a unique sequence of $z_n \in C_n^a$ with this spiraling behavior. z_n is the central vertex of the dynamical frame $\mathcal{F}_n^a(u_n,\, v_n)$.

In [14] we shall see that there is a cobweb of "p-curves" around a, joining these centers, and a similar cobweb for $\mathcal{K}_a$. These curves are yet another structure that provides a (qualitative) similarity between the parameter plane and the dynamical plane around a.

Proof of Lemma 8: For $\{z_n\}$, existence and uniqueness are clear from the structure of the hierarchies on the incident arcs (Theorem 4, Figure 6). Remember the uniqueness statement in paragraphs 1 and 2 of Lemma 3. To obtain the parameters u_n and v_n, either solve the linear recursion (12), or note that ϕ and ψ' or ψ and ϕ' of (9) are external angles of a. In the parameter plane, c_4, c_7, c_{10}, ... and c_5, c_8, c_{11}, ... are obtained from the frames $\mathcal{F}_n^M(u_n,\, v_n)$ with Theorem 6.
For $n = 3,\, 6,\, 9,\, \ldots$, define $\theta_n = \dfrac{u_n}{2^n-1}$ and $\theta_n' = \dfrac{v_n}{2^n-1}$. The angles θ_n and θ_n' have been obtained from the parameters of dynamical frames, but it is not obvious that they land at the same component and that it has the period n, since Lemma 7 is weaker than Theorem 6. The proof is by induction: Assume that θ_n and θ_n' land at the root of the period-n component with the center c_n. Period-doubling yields the angles $.\overline{u_n v_n}$ and $.\overline{v_n u_n}$. Now $\dfrac{9}{56} - .\overline{u_n v_n} = \dfrac{1}{56\cdot(2^n+1)} < \dfrac{1}{2^{n+3}-1}$, thus $\mathcal{R}_M(\theta_{n+3})$ is the only ray with a period $\le n+3$, that may land on the arc from c_n to a from the right, and $\mathcal{R}_M(\theta_{n+3}')$ is the only one on the left. Thus they land at the same root, belonging to a center c_{n+3} of period dividing $n+3$. Now $\theta_{n+3} = .\overline{001\,010\,010\,\ldots\,010}$, thus the period is $n+3$. ∎
This proof (in the simpler case for $c_4, \ldots, c_5, \ldots$) extends to all vertices of the graph of $\mathcal{M}_{1/3}$, but the analytical proofs of [8] and [10] apply to every Misiurewicz point in $\mathcal{M}$. If $b \in V_n^M$, our proof shows that the smallest period on the edges incident to b is n.
Let θ, θ_1 etc. denote the standard angles of the frame $\mathcal{F}_n^M(u_n,\, v_n)$ for $n = 4,\, 7,\, \ldots$. The external angle of the $\mathcal{M}_{1/3}$-tip $1/4 = .00\overline{1} = .01\overline{0}$ is tuned by c_n to $\tau_1 = .uu\bar{v}$ and $\tau_2 = .uv\bar{u}$. We have $\theta_2 - \theta_1 = \frac{1}{28}\, 2^{-n}$, $\theta_3 - \theta_2 = \frac{1}{14}\, 2^{-n}$ and $\tau_2 - \tau_1 \sim \frac{1}{14}\, 2^{-n}$. These intervals belong to arms of the frame, while the tuned copy of $\mathcal{M}$ is contained in $\tau_1 - \theta_2 \sim \frac{1}{8}\, 2^{-2n}$ and $\theta_3 - \tau_2 \sim \frac{5}{56}\, 2^{-2n}$. This scaling is analogous to the result of Eckmann–Epstein on the diameter in the parameter plane.
If $\mathcal{M}$ is locally connected, the conformal mapping $\Phi_M^{-1} : \mathbb{C} \setminus \overline{\mathbb{D}} \to \mathbb{C} \setminus \mathcal{M}$ will

have a continuous extension to the boundary. Φ_M^{-1} will be Hölder continuous at the preimages of a with exponent $\dfrac{\log|\rho_a|}{\log 2} = .4096137284$. It is well known that it will not be Hölder continuous at a Feigenbaum point.

9 The Structure of the Frames and some Orbits

9.1 Some critical orbits

Suppose that $\mathcal{F}_n^M(u, v)$ is a parameter frame on the edge $\mathcal{E}_M$ from a to $\gamma_M(23/112)$. The center of period n shall be c, and θ_i, θ_i' denote the standard angles. The orbit of c is described as follows: For $k = 3, 6, 9, \ldots, n-1$, $f_c^k(c)$ belongs to the edge from α_c to $-\alpha_c$. For $k = 4, 7, 10, \ldots, n-3$, $f_c^k(c)$ belongs to the edge from α_c to $\gamma_c(9/56)$, and for $k = 5, 8, 11, \ldots, n-2$, it belongs to the edge from α_c to $\gamma_c(9/28)$.
To c we associate an itinerary (see Section 5), a finite sequence of symbols $s_3, s_6, \ldots, s_{n-4}, *$ with $s_k = l$ or $s_k = r$, if $f_c^k(c)$ is between α_c and 0 or between 0 and $-\alpha_c$, respectively. The hierarchy of parameter frames on $\mathcal{E}_M$ corresponds to the hierarchy of all possible itineraries. Note that the edge from α_c to $-\alpha_c$, excluding $\mathcal{F}_1^c(1, 0)$, is mapped 2–1 onto the whole edge by f_c^3, in the same fashion as $\mu x(1-x)$ with $\mu > 4$ maps the unit interval. In the latter case, itineraries are well-known on the invariant Cantor set, but we use them to characterize the intervals in-between.
For $1 \le k \le n-1$ and $c' \in \mathcal{F}_n^M(u, v)$, $f_{c'}^k$ maps $\mathcal{F}_n^{c'}(u, v)$ bijectively onto some dynamical frame, especially $f_{c'}^{n-1} : \mathcal{F}_n^{c'}(u, v) \to \mathcal{F}_1^{c'}(1, 0)$. For $c' = \gamma_M(\theta_1)$ or $c' = \gamma_M(\theta_3)$, we have $f_{c'}^{n-1}(c') = \gamma_{c'}(9/112)$ or $f_{c'}^{n-1}(c') = \gamma_{c'}(15/112)$. Thus $f_{c'}^n(c') = \gamma_{c'}(9/56)$, and $f_{c'}^{n+3}(c') = \alpha_{c'}$.

9.2 Secondary frames

For all c in the left branch of $\mathcal{M}_{1/3}$, a dynamical frame $\mathcal{F}_n^c(u, v)$ has the same external angles θ_i, θ_i'. In this sense, the frame does not undergo a bifurcation. A frame contains smaller frame-like subsets which do bifurcate, and we shall now describe a special case, which is illustrated in Figure 10. Denote by $\mathcal{E}_M$ the edge from a to $b := \gamma_M(23/112)$ and suppose that $\mathcal{F}_n^M(u, v)$ is a parameter frame in $\mathcal{E}_M$ with the characteristic angles θ_i, θ_i'. The dynamical frame $\mathcal{F}_1^c(1, 0)$ is mapped 2–1 by f_c onto the part of $\mathcal{K}_c$ between $\mathcal{R}_c(9/56)$ and $\mathcal{R}_c(15/56)$. Especially, it contains the preimages of $\mathcal{F}_n^c(u, v)$. If these form two frame-like subsets, these shall be called secondary (dynamical) frames.
Figure 10 shows the bifurcation of secondary frames as c moves through $\mathcal{E}_M$ from a to b. Intuitively, the horizontal part of $\mathcal{F}_1^c(1, 0)$ is stretched while the vertical part is shrinked. The secondary frames move from the vertical part to the horizontal part, and their characteristic external angles undergo a bifurcation at $c = \gamma_M(\theta_1)$ and $c = \gamma_M(\theta_3)$. For c in the middle part of $\mathcal{F}_n^M(u, v)$, between the two Misiurewicz points, the preimage of $\mathcal{F}_n^c(u, v)$ is one connected subset in the middle of

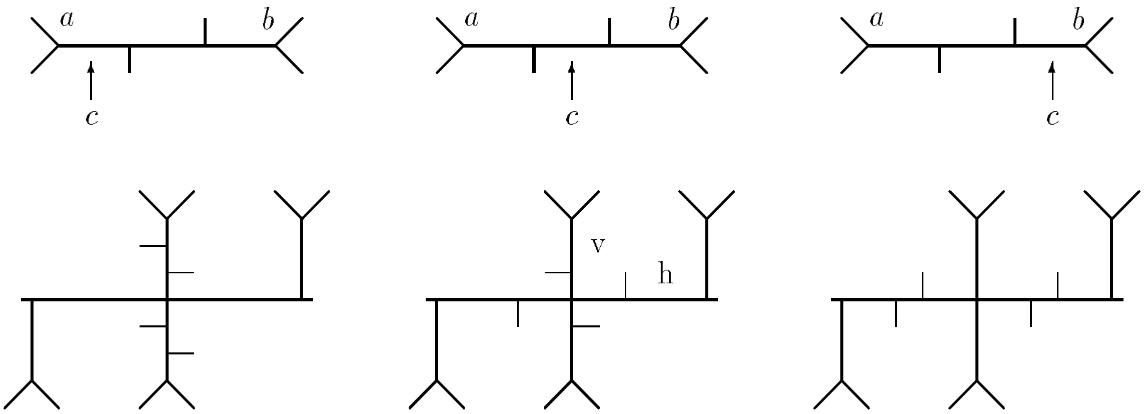

Figure 10: Bifurcations of secondary frames as c varies in $\mathcal{E}_M$.

$\mathcal{F}_1^c(1,\,0)$. Now the region marked "h" in Figure 10 consists of secondary frames, that are preimages of frames between $\gamma_c(11/56)$ and $\gamma_c(\theta_1)$, and the region marked "v" consists of secondary frames that are preimages of frames between $\gamma_c(\theta_3)$ and $\gamma_c(23/112)$. These secondary frames do not bifurcate for c between $\gamma_M(\theta_1)$ and $\gamma_M(\theta_3)$, and corresponding subframes exist in every dynamical frame, especially in $\mathcal{F}_n^c(u,\,v)$.

Thus they correspond to secondary parameter frames in $\mathcal{F}_n^M(u,\,v)$. Especially, $\mathcal{F}_4^M(3,\,4)$ contains a family of secondary frames on the arc from $\gamma_M(179/896)$ to $\gamma_M(2865/14336)$, and another one on the arc from $\gamma_M(2871/14336)$ to $\gamma_M(359/1792)$. Both families form complete hierarchies, with one secondary frame of order 11, two of order 14, four of order 17,... . If $\mathcal{F}_n^M(u,\,v) \neq \mathcal{F}_4^M(3,\,4)$, at least one of the two corresponding families does not form a hierarchy in this sense.

The arc from $\gamma_M(179/896)$ to the root $\gamma_M(3/15)$ consists of an infinite family of arcs accumulating at the root, each of which contains a hierarchy of frame-like subsets. The largest periods are 11, 15, 19, ... $c' := \gamma_M(769/3840)$ is obtained by tuning $\gamma_M(1/4)$ by the period-4 center c_4. The arc from c' to $\gamma_M(359/1792)$ contains a similar family of hierarchies, accumulating at c'. Presumably, this is true for every c_4-tuned tip of $\mathcal{M}$.

9.3 Frames on different edges

This section is still under construction.

Lemma 9 *Arms of a frame in the left branch can be described as follows: The arms "before" $\gamma_M(\theta)$ correspond to arms of the graph of $\mathcal{M}_{1/3}$ on the way from $\gamma_M(1/7)$ to the current edge.*

In the example of the frame in the right part of Figure 7 on page 20, there is one arm pointing to the right (ending at $\gamma_M(\eta_1)$), and then one arm pointing to the left (ending at $\gamma_M(\eta_2')$. If we travel through the graph to the current edge, there is one arm pointing to the right at a, and then one arm pointing to the left at $\gamma_M(23/112)$.

Analogous results hold for the right branch, cf. Figure 8.

The correspondence between the frame and the graph is established by considering preimages of a dynamical frame within itself, as in the discussion of secondary frames in Section 9.2.

10 The 1/2-Limb

This section is still under construction.

Para-puzzles are defined for every limb $\mathcal{M}_{k/m}$, and the corresponding recursion for external angles is obtained from the angles of $\pm\alpha_c$. The graph of $\mathcal{M}_{k/m}$ has m edges at every vertex, and the frames form a hierarchy, where the order is increased by m at every level.

In the case of $\mathcal{M}_{1/2}$, the largest edge connects $\gamma_M(5/12)$ and $\gamma_M(11/24)$. It contains one frame of order 3, two frames of order 5, four of order 7 ..., and this hierarchy implies Sharkovsky's ordering for the cycles of a real quadratic polynomial. By considering the orbits of the characteristic Misiurewicz points, we show that the Branner–Douady homeomorphism Φ_A [1] maps these frames into frames of $\mathcal{M}_{1/3}$, respecting the hierarchical structure.

We get an idea of the location of all hyperbolic intervals on the real axis: Every edge contains a hierarchy of frames, every frame contains a "window" and families of hierarchies of secondary frames, and every window contains tuned copies of edges.

Part II: Surgery

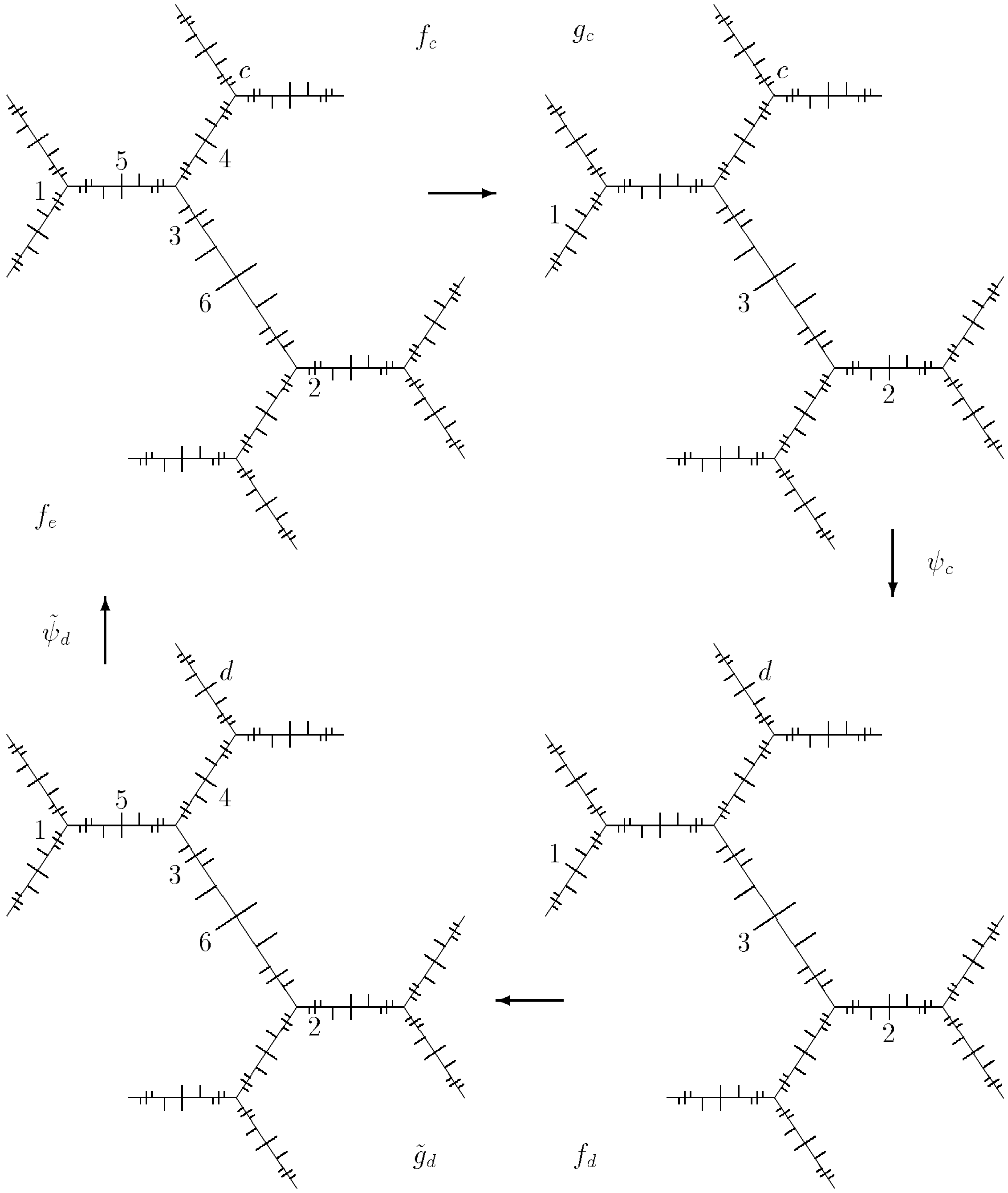

Figure 11: Examples of the surgical procedure, with $c = e \in \mathcal{F}_7^M(25, 34)$ and $d \in \mathcal{F}_4^M(3, 4)$. The homeomorphisms are $d = h(c)$ and $e = \tilde{h}(d)$. See the explanation before Theorem 10.

11 Introduction to Quasi-conformal Surgery

11.1 Quasi-conformal mappings

Suppose that an orientation-preserving homeomorphism $\phi : D \to D'$ is weakly differentiable. The derivative $D\phi$ maps infinitesimal ellipses onto circles, and the ellipse field can be described by the Beltrami coefficient $\mu(z) = \frac{\overline{\partial}\phi(z)}{\partial\phi(z)}$ [5]. If the dilation ratio of the ellipses is bounded by $\mathcal{K} \geq 1$, ϕ is K-quasi-conformal. Equivalently, $\mu(z)$ is bounded by $M = \frac{K-1}{K+1} < 1$ almost everywhere. If f is conformal, then $f \circ \phi$ and $\phi \circ f$ are again K-quasi-conformal. ϕ is conformal, iff $K = 1$, or $\mu = 0$. A mapping of the form $f \circ \phi$ with f holomorphic and ϕ quasi-conformal is called quasi-regular.

Measurable Riemann Mapping Theorem by Ahlfors-Behrs
Denote the unit disk by $\mathbb{D}$. If D is a bounded, simply connected domain and $\mu : D \to \mathbb{C}$ is a measurable Beltrami coefficient with $|\mu(z)| \leq M < 1$, there is a quasi-conformal homeomorphism $\phi : D \to \mathbb{D}$ with $\frac{\overline{\partial}\phi}{\partial\phi} = \mu$, thus ϕ maps the ellipse field to circles. ϕ is unique up to a Möbius transformation $\mathbb{D} \to \mathbb{D}$.

Convergence Theorem (see [20])
Suppose that $\phi_j : \mathbb{D} \to D_j$ are K-quasi-conformal and the regions D_j are uniformly bounded. Then there is a subsequence $\phi_{j'}$ and a mapping $\phi : \mathbb{D} \to \mathbb{C}$ with $\phi_{j'} \to \phi$ pointwise. The kernel of $\{D_j\}$ contains all points z, such that a neighborhood of z belongs to almost all D_j. Now there are two possibilities: Either $\phi : \mathbb{D} \to D'$ is K-quasi-conformal, D' is a component of kernel$(D_{j'})$, and the convergence is uniform on compact subsets of $\mathbb{D}$. Or $\phi \equiv \text{const} \in \mathbb{C} \setminus (\text{kernel}(D_{j'}) \cup \text{kernel}(\mathbb{C} \setminus \overline{D_{j'}}))$. In the first case, $\phi_{j'}^{-1} \to \phi^{-1}$ uniformly on compact subsets of D'. If all $D_j = D_0$, then $D' = D_0$ in the first case, and const $\in \partial D_0$ in the second case.

11.2 Quasi-conformal surgery

There are two basic ideas in the application of quasi-conformal mappings to iteration theory:

- Suppose that g is quasi-regular and we want to obtain a holomorphic function h with the same dynamics. If an ellipse field μ is invariant under g (i.e. under the tangent map $T_z g$) and the dilation ratio is bounded, we construct ϕ with the Measurable Riemann Mapping Theorem and set $h := \phi \circ g \circ \phi^{-1}$. Then h maps infinitesimal circles to circles, thus it is holomorphic.

- Typically g is defined piecewise, it equals different holomorphic functions in certain subsets of its domain, and is quasi-regular in small sectors or annuli between these subsets. Denote these regions of non-holomorphy by T', and $T'' = \bigcup_{n=1}^{\infty} g^{-n}(T')$. If no component of $T' \cup T''$ is periodic, an g-invariant ellipse field μ can be constructed recursively, by setting $\mu = \frac{\overline{\partial}g}{\partial g}$ in T' and defining the ellipses in $g^{-n}(T')$ so that they are mapped to those in $g^{-(n-1)}(T')$ by $T_z g$. This is called Shishikura's principle.

Quasi-conformal surgery has had many applications e.g. by Sullivan and Shishikura. See the reviews and references in [5, 9].

11.3 Polynomial-like mappings

The theory of polynomial-like mappings was developed by Douady and Hubbard in [8]. A holomorphic function $f : U_1 \to U_2$ is called *polynomial-like* of degree d, if it is proper of degree d and $\overline{U_1} \subset U_2$. $\mathcal{K}_f := \{z \in U_1 \,|\, f^n(z) \in U_1 \text{ for } n \in \mathbb{N}\}$ is the filled Julia set. If $\tilde{f} : \tilde{U}_1 \to \tilde{U}_2$ is polynomial-like, f and $\tilde{f}$ are called *quasi-conformally equivalent*, $f \overset{\text{qc}}{\sim} \tilde{f}$, if there is a quasi-conformal mapping χ with $\chi \circ f \circ \chi^{-1} = \tilde{f}$ in a neighborhood of $\mathcal{K}_{\tilde{f}}$. They are *hybrid-equivalent*, $f \overset{\text{hb}}{\sim} \tilde{f}$, if $\overline{\partial}\chi$ vanishes almost everywhere on $\mathcal{K}_f$.

The **Straightening Theorem** says:

A polynomial-like map f of degree d is hybrid-equivalent to a polynomial P of degree d. If $\mathcal{K}_f$ is connected, then P is unique up to an affine conjugation (for $d = 2$, we may set $P = z^2 + c$ for a unique $c \in \mathcal{M}$).

Moreover, if $c \in \partial\mathcal{M}$ and $\tilde{c} \in \mathcal{M}$ with $f_c \overset{\text{qc}}{\sim} f_{\tilde{c}}$, then $c = \tilde{c}$.

If f_c^n is polynomial-like of degree 2 in some set, it corresponds to a unique f_d. The mapping $c \mapsto d$ in parameter space is obtained by renormalization. If c was obtained from tuning c_0 by a hyperbolic component of period n, then $d = c_0$. By considering analytical families of polynomial-like mappings, Douady and Hubbard explain that small copies of $\mathcal{M}$ appear in $\mathcal{M}$ and in other parameter spaces.

11.4 The homeomorphisms of Branner–Douady and Branner–Fagella

In [1], Branner and Douady construct a homeomorphism Φ_A of $\mathcal{M}_{1/2}$ onto a subset of $\mathcal{M}_{1/3}$, and a homeomorphism Φ_B of $\mathcal{M}_{1/2}$ onto a limb in some cubic parameter space. In [4], Branner and Fagella construct a homeomorphism of $\mathcal{M}_{p/q}$, $q \geq 3$, onto a limb of the connectedness locus of $\lambda z(1+z/q)^q$, and by composition $\Phi^q_{pp'} : \mathcal{M}_{p/q} \to \mathcal{M}_{p'/q}$ is obtained. The "first return map" g is constructed from f in two ways (*topological surgery*):

- Some pieces of the dynamical plane are cut out, and in the remaining pieces, g equals some iterate f^n, where n is minimal such that the image belongs to the truncated space.

- Some pieces are added, and g is the identity between copies of the same piece.

In both cases, the resulting Riemann surface is mapped to a domain in $\mathbb{C}$, and g is smoothed in sectors around some external rays where a shift discontinuity occurred (*quasi-conformal surgery*). A holomorphic function is obtained by the method of Section 11.2 (*holomorphic surgery*). This function is hybrid-equivalent to a unique polynomial in the desired family, by the suitable construction of g. The resulting mapping between parameter spaces is shown to be a homeomorphism. In [4], the proofs are given in greater detail, and additional results on the induced mapping of external arguments are obtained (*combinatorial surgery*).

12 Mapping Frames by Quasi-Conformal Surgery

We use quasi-conformal surgery similar to that of Branner–Douady [1] and Branner–Fagella [4]. The main differences are:

- We do not need to consider polynomials of degree > 2.
- We do not add pieces to or remove pieces from the dynamical plane, but stay in $\mathbb{C}$. Some pieces are stretched and others are shrinked, so that they fit together again.
- Our construction of the "first return map" g is different, since we cannot set $g = f^n$ on some pieces: Suppose that we require g to map $\mathcal{U} \to \mathcal{U}'$, and that there are $m, n \in \mathbb{N}$ with $f^m(\mathcal{U}) = \pm f^n(\mathcal{U}')$. Then we set $g = (f^n_{|\mathcal{U}'})^{-1} \circ (\pm f^m)$ on $\mathcal{U}$, or $g = f^{-n} \circ (\pm f^m)$ for short. If $m - n > 1$, we say that g is faster than f, periods will be reduced, and $\mathcal{U}' = g(\mathcal{U})$ will in some sense be "larger" than $f(\mathcal{U})$. Conversely, if $m - n < 1$, then g is slower than f, periods are increased, and $\mathcal{U}' = g(\mathcal{U})$ is smaller than $f(\mathcal{U})$.

Thus we introduce a new method to obtain the first return map, but the technical details are similar to [4]. The construction of the regions U_1, U_2 is more involved (see Section 13.3), and we use a different technique for smoothing g in sectors (see Section 13.4).

We consider parameters c in the edge $\mathcal{E}_M$ from a to $b = \gamma_M(23/112)$. The strip around the corresponding critical edge from $\gamma_c(11/56)$ to $\gamma_c(23/112)$ in the dynamical plane is cut into three pieces, as it is sketched in Figure 12 on page 35. Now f_c is replaced by g_c, which is of the form $f_c^{-n} \circ (\pm f_c^m)$ in these three pieces. As an example, note that $\mathcal{U}_c'$ is larger than $\mathcal{U}_c$, and $f_c^3(\mathcal{U}_c') = f_c^6(\mathcal{U}_c)$. (It will be convenient to set $g_c = f_c \circ j_c$ and to describe j_c in detail.) j_c is stretching $\mathcal{U}_c$ to $\mathcal{U}_c'$, shifting $\mathcal{V}_c$ to $\mathcal{V}_c'$, and shrinking $\mathcal{W}_c$ to $\mathcal{W}_c'$. In this way, a preliminary function $g_c^{(1)}$ is obtained, which is defined in $\mathbb{C}$ except on eight dynamical rays, where a shift discontinuity occurs. Now $g_c^{(1)}$ is restricted to a bounded domain and smoothed in eight sectors. The resulting function g_c is transformed to a holomorphic function by constructing a g_c-invariant ellipse field, and the Straightening Theorem yields a hybrid equivalence $\psi_c \circ g_c \circ \psi_c^{-1} = f_d$ with $d \in \mathcal{E}_M$. The mapping $h : \mathcal{E}_M \to \mathcal{E}_M$ is defined by setting $h(c) := d$, and it is shown to be a homeomorphism.

Similar homeomorphisms can be obtained by cutting not on the critical edge but on its first or second image. Our choice has the advantage that ψ_c maps the dynamical frames in the same way as j_c does. Now h maps parameter frames on $\mathcal{E}_M$ in the same way as ψ_c or j_c map the dynamical frames on the critical edge. Especially, h maps $\mathcal{F}_7^M(25,\, 34)$ onto $\mathcal{F}_4^M(3,\, 4)$, and we can show that all frames on $\mathcal{E}_M$ are homeomorphic. Neglecting the exceptional set, $\mathcal{E}_M$ consists of a countable family of homeomorphic subsets.

Consider the example in Figure 11 on page 28. c is the center of period 7 in $\mathcal{F}_7^M(25,\, 34)$, and the critical orbit under f_c is sketched in the upper left part. In the upper right part, the orbit under g_c is sketched. c belongs to the part $\mathcal{U}_c$ of the critical edge that is stretched by j_c, and we have $g_c(c) \neq f_c(c)$ and $g_c^2(c) \neq f_c^2(c)$, but $g_c^3(c) = f_c^6(c) = 0$. Thus g_c has a super-attracting 4-cycle. Setting $\psi_c \circ g_c \circ \psi_c^{-1} = f_d$ with $h(c) = d$, we see that d is the center of $\mathcal{F}_4^M(3,\, 4)$. The orbit of d under f_d is sketched in lower right part. Note that ψ_c maps frames in the same way as j_c. A different homeomorphism $\tilde h$ is constructed from $\tilde\jmath_d$ and $\tilde g_d$. The new parameter d belongs to $\mathcal{U}_d'$ which is shrinked by $\tilde\jmath_d$, thus $\tilde g_d$ has again a super-attracting 7-cycle as sketched in the lower left part. By conjugating with $\tilde\psi_d$, we obtain f_e and set $\tilde h(d) = e$. We will show that $e = c$, thus h and $\tilde h$ are inverse mappings.

Theorem 10 *Denote by $\mathcal{E}_M$ the edge from $a = \gamma_M(11/56)$ to $b = \gamma_M(23/112)$. The mapping $h : \mathcal{E}_M \to \mathcal{E}_M$ is constructed by quasi-conformal surgery.*

1. *h is a homeomorphism of $\mathcal{E}_M$ onto itself, fixing a and b. For $d = h(c)$, there is a quasi-conformal homeomorphism ψ_c with $\mathcal{K}_d = \psi_c(\mathcal{K}_c)$.*

2. *h is mapping frames onto frames, e.g.*
$\mathcal{F}_{10}^M(201,\, 274) \to \mathcal{F}_7^M(25,\, 34) \to \mathcal{F}_4^M(3,\, 4) \to \mathcal{F}_7^M(26,\, 33) \to \mathcal{F}_{10}^M(210,\, 265)$.

3. *h is holomorphic in the interior of $\mathcal{E}_M$. If Ω is a hyperbolic component of period p in $\mathcal{E}_M$, then $h(\Omega)$ is a hyperbolic component of period q with $\frac{4}{7}p \le q \le \frac{7}{4}p$.*

4. *h is compatible with tuning.*

See Theorem 13 on page 43 for results on the induced mapping of external angles and the practical computation of $h(c)$. Some generalizations are stated in Section 17: All the frames on the same edge are homeomorphic, and similar results are obtained on all edges of $\mathcal{M}_{1/3}$, and for all limbs $\mathcal{M}_{k/m}$.

Our first motivation for defining the parameter frames was that they correspond to six-stars in $\mathcal{K}_a$, both by their external arguments, and by Tan Lei's asymptotic similarity. In Section 7, some common structure of the frames was revealed on the combinatorial level, and now we see that they are in fact homeomorphic. This forms a complement to the statement that $\rho_a^k(\mathcal{F}_k^M(u_k,\, v_k) - a)$ has a limit for $k = 4,\, 7,\, 10,\, \ldots \to \infty$ (see Section 8 for the notation). The homeomorphism h can be considered as yielding dynamics to $\mathcal{E}_M$. It corresponds qualitatively to the mapping F_a^3 with $F_a = f_a^{-3} \circ f_a \circ f_a^3$ around $a \in \mathcal{K}_a$, on the dynamical edge from $\gamma_a(11/56)$

to $\gamma_a(23/112)$. While $F_a'(a) = \rho_a$ implies the asymptotic self-similarity of $\mathcal{K}_a$, we cannot prove the corresponding result on $\mathcal{M}$ from properties of h. Conversely, we expect that the scaling properties of Section 8 imply $h(c) \sim a + \rho_a^3(c-a)$ for $c \to a$, $c \in \mathcal{E}_M$.

Proof of Theorem 10:

1. We give the details of the construction in Section 13, show in Section 14 that h is bijective, and in Section 15 that h is continuous.
2. Suppose that c_0 is the center of some parameter frame and θ_i, $\tilde{\theta}_i$ are the standard angles. We have described the structure of some orbits in Section 9.1, and we see that both c_0 and the Misiurewicz points $\gamma_M(\theta_i)$ are mapped by h to the corresponding points in another frame. Thus the connected components defined by the Misiurewicz points are mapped in the same way.

A second proof is as follows: For $d = h(c)$ and ψ_c according to Section 13.7, we have the following property: If j_c maps $\mathcal{F}_n^c(u,\, v) \to \mathcal{F}_{n'}^c(u',\, v')$, then ψ_c maps $\mathcal{F}_n^c(u,\, v) \to \mathcal{F}_{n'}^d(u',\, v')$, and this relation between dynamical frames is independent of c. Thus $c \in \mathcal{F}_n^c(u,\, v) \Leftrightarrow d \in \mathcal{F}_{n'}^d(u',\, v')$, since $d = \psi_c(c)$. Note that $c \in \mathcal{F}_n^c(u,\, v) \Leftrightarrow c \in \mathcal{F}_n^M(u,\, v)$ and analogously for d.

3. See Sections 13.5, 15.1 and 15.2.
4. See the proof of the corresponding result in [4, Section 5.7].

13 Construction of the Homeomorphism h

13.1 Sectors around external rays

For $c \in \mathcal{M}_{1/3}$, consider the conformal mapping $\Phi_c : \mathbb{C} \setminus \mathcal{K}_c \to \mathbb{C} \setminus \overline{\mathbb{D}}$, and the Green's function $G_c(z) = \log|\Phi_c(z)|$. For $z \in (\mathbb{C} \setminus \mathcal{K}_c) \setminus \mathcal{R}_c(0)$ write $\Phi_c(z) = \mathrm{e}^{w}$ with $w = \rho + 2\pi i t$. The mapping $w \mapsto z$ is a bijection, when we choose the halfstrip $\{w \,|\, \rho > 0,\ 0 < t < 1\}$ as its domain (alternatively, one could consider an infinite covering of $\mathbb{C} \setminus \mathcal{K}_c$ by the right halfplane). Define the sector

$$S_n(\theta) = \Big\{ w = \rho + 2\pi i t \,\Big|\, 0 < \rho < \frac{\eta}{2^n},\ -s\rho < t - \theta < s\rho \Big\} \qquad (14)$$

for suitable $n \in \mathbb{N}_0$ and $s,\, \eta > 0$, and $S_n^c(\theta) := \Phi_c^{-1}(\exp S_n(\theta))$. If $\theta \in \mathbb{Q}$, the dynamical ray $\mathcal{R}_c(\theta)$ terminates at $z_0 := \Phi_c^{-1}(\exp 2\pi i\theta) := \gamma_c(\theta)$, and if $w_j \in \overline{S_n(\theta)}$ with $w_j \to 2\pi i\theta$, then $\Phi_c^{-1}(\exp w_j) \to z_0$ by Theorem 2.2 in [5]. This implies $\overline{S_n^c(\theta)} = \Phi_c^{-1}(\exp \overline{S_n(\theta)})$, and $S_n^c(\theta)$ is a distorted sector with vertex z_0.

Now f_c is conjugate to multiplication by 2 in the strip (with w modulo $2\pi i$, or t modulo 1). Thus $f_c^{-1}(S_n^c(\theta)) = S_{n+1}^c(\frac{\theta}{2}) \cup S_{n+1}^c(\frac{\theta+1}{2})$. For fixed $s,\, \eta > 0$ with $s\eta < 1/14$, define $S_0^c := S_0^c(1/7) \cup S_0^c(2/7) \cup S_0^c(4/7)$, $S_1^c := S_1^c(9/14) \cup S_1^c(11/14) \cup S_1^c(1/14)$, and $S_{n+1}^c := f_c^{-1}(S_n^c)$ for $n \in \mathbb{N}$. Then S_n^c contains one sector around each external ray landing at a $z \in A_n^c$ (preimages of α_c of order n). All sectors in $S^c := \bigcup\limits_{n=0}^{\infty} S_n^c$ are disjoint: For $w = \rho + 2\pi i t$ with $0 < \rho < \eta$ and $0 < t < 1$, there is a unique $n_0 \in \mathbb{N}_0$ with $\frac{\eta}{2^{n_0+1}} \le \rho < \frac{\eta}{2^{n_0}}$, and w does not belong to $\bigcup\limits_{n=n_0+1}^{\infty} S_n^c$. The sectors in $\bigcup_{n=0}^{n_0} S_n^c$ have $\theta = \dfrac{k}{7 \cdot 2^{n_0}}$ with $k \in I\!N$, and they do not overlap for $\rho < \dfrac{\eta}{2^{n_0}}$, since $2s\rho < \dfrac{1}{7 \cdot 2^{n_0}}$.

Consider the orbit of a $z \in \mathbb{C} \setminus \mathcal{K}_c$. If it passes through S^c, there is a smallest $k \in I\!N_0$ with $f_c^k(z) \in S^c$, thus $f_c^k(z) \in S_n^c$ for a unique n. Then $f_c^{k+1}(z) \in S_{n-1}^c, \ldots, f_c^{k+n}(z) \in S_0^c$, and the orbit stays in S_0^c for a finite number of iterations. Afterwards it travels through $G_c(\cdot) \geq \eta$, thus it has left S^c forever. Especially, no sector in $S^c \setminus S_0^c$ is visited twice.

13.2 Preliminary definition of g_c

We consider parameters c in the edge $\mathcal{E}_M$ from $a = \gamma_M(11/56)$ to $b = \gamma_M(23/112)$. In the dynamical plane for f_c, the critical value c belongs to the edge from $\gamma_c(11/56)$ to $\gamma_c(23/112)$. The corresponding strip (the puzzle-piece 1200120) is written as a union of three strips $\mathcal{U}_c$, $\mathcal{V}_c$ and $\mathcal{W}_c$ as sketched in the bottom of Figure 12. Now f_c is replaced by $g_c = f_c \circ j_c$, where $j_c(z) = z$ in most parts of the plane. Here we a give a preliminary definition $g_c^{(1)} = f_c \circ j_c^{(1)}$. We have

$$j_c^{(1)}(z) \;=\; \begin{cases} f_c^{-3} \circ f_c^{6} & , \quad z \in \mathcal{U}_c \\ f_c^{-9} \circ (-f_c^{9}) & , \quad z \in \mathcal{V}_c \\ f_c^{-6} \circ (-f_c^{3}) & , \quad z \in \mathcal{W}_c \\ z & , \quad \text{otherwise}, \end{cases} \tag{15}$$

where e.g. f_c^{-3} means $(f^3_{c\,|\mathcal{U}_c'})^{-1}$. Now $j_c^{(1)}$ maps $\mathcal{U}_c \to \mathcal{U}_c'$, $\mathcal{V}_c \to \mathcal{V}_c'$ and $\mathcal{W}_c \to \mathcal{W}_c'$, where these sets are defined in the top of Figure 12. So far, $j_c^{(1)}$ and $g_c^{(1)}$ are not defined on the eight dynamical rays bounding the strips, and they will have shift discontinuities there. In Section 13.4 we will modify the definition in sectors around these rays to obtain a smooth mapping. We work in the w-halfstrip, and we shall give an example of a shift discontinuity using the variable w: The mapping $J^{(1)}$ conjugate to $j_c^{(1)}$ sends

$$\begin{aligned} \rho + 2\pi i\,(1415/7168 - 0) \;&\mapsto\; 8\rho + 2\pi i\, 183/896 \quad \text{and} \\ \rho + 2\pi i\,(1415/7168 + 0) \;&\mapsto\; \rho + 2\pi i\, 183/896 \;, \end{aligned}$$

thus there is a shift along the ray of discontinuity, which can be smoothed out. Note that $f_c^{-6} \circ f_c^{6}$ maps $\mathcal{V}_c$ onto $\mathcal{V}_c'$, but it includes a "rotation of 180°": $\rho + 2\pi i\,(1415/7168 + 0)$ is mapped to $\rho + 2\pi i\, 1863/7168$. We cannot take this as the definition of $j_c^{(1)}$ in $\mathcal{V}_c$, since the resulting discontinuity could not be smoothed.

13.3 Preliminary definition of the domains

We will construct domains U_1^c, U_2^c such that $\overline{U_1^c} \subset U_2^c$ and g_c is a 2–1 proper mapping $U_1^c \to U_2^c$. The curves ∂U_1^c and ∂U_2^c are best described in the variable $\Phi_c(z)$ or $w = \log \Phi_c(z) = \rho + 2\pi i t$. Here the curves ∂U_i will be defined by discontinuous

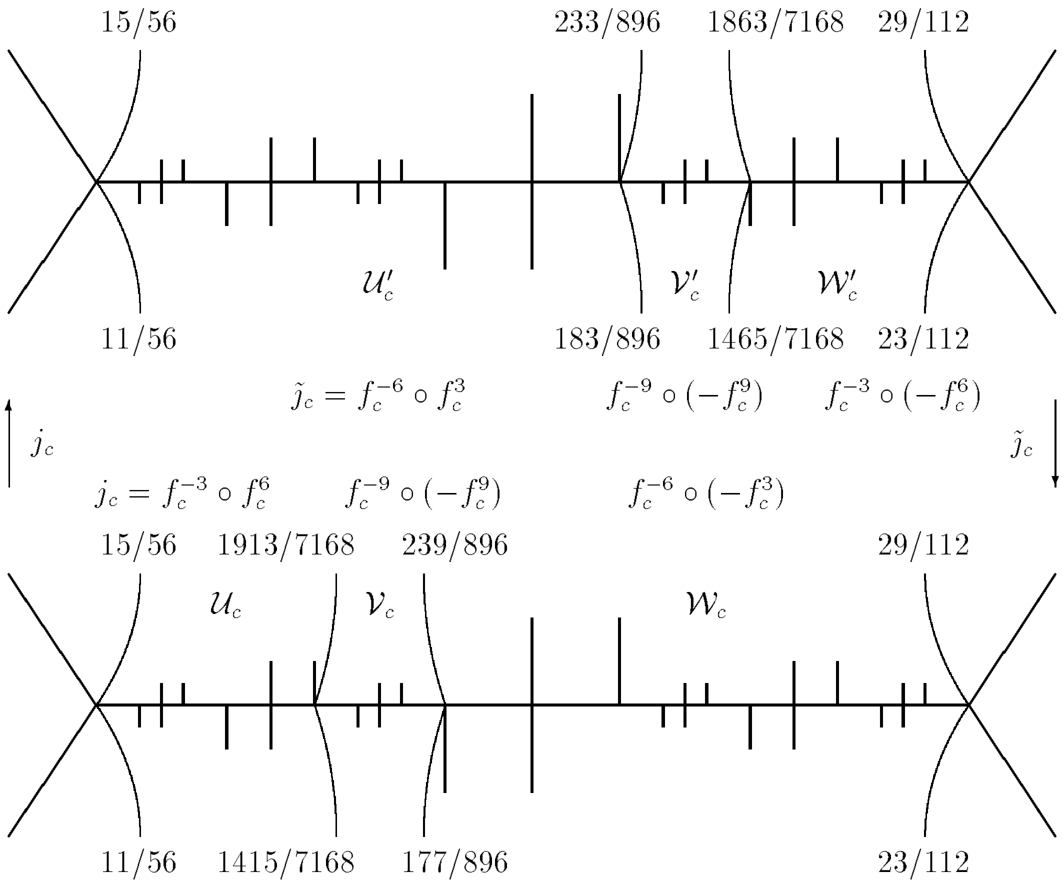

Figure 12: Decompositions of the edge from $\gamma_c(11/56)$ to $\gamma_c(23/112)$ and definition of the mappings j_c (15) and $\tilde{\jmath}_c$ (17). The mapping $g_c = f_c \circ j_c$ with e.g. $g_c : \mathcal{U}_c \to f_c(\mathcal{U}_c')$ can be visualized by the same picture. The corresponding mappings of external arguments are obtained by dividing the mappings in (18) and (19) by 2.

functions $\rho = \rho_i(t)$, and the step discontinuities will be smoothed in Section 13.4 (we do not write $U_i^{c(1)}$ for simplicity). We shall use sectors with fixed s, $\eta > 0$ satisfying $s\eta < 1/14$. For most angles $t \in [0, 1)$, we have $\rho_1(t) = \eta/2^{11}$ and $\rho_2(t) = \eta/2^{10}$, thus $\partial U_i^c = \Phi_c^{-1}(\exp \partial U_i)$ is a level curve of G_c. For $z \in \mathcal{U}_c$, thus $11/56 < t < 1415/7168$ and $1913/7168 < t < 15/56$, we set $\rho_1(t) = \eta/2^{14}$, in order to have this part of ∂U_1^c mapped into ∂U_2^c by $f_c^{-2} \circ f_c^6$. Next we set $\rho_1(t) = \eta/2^8$ and $\rho_2(t) = \eta/2^{7.75}$ for $177/896 < t < 23/112$ and $29/112 < t < 239/896$, thus $z \in \mathcal{W}_c$ (the value $\eta/2^7$ seems more natural, but it would cause some problems). Now ∂U_2^c was pushed out in $\mathcal{W}_c$, and we must define ∂U_i^c in $g_c^{-1}(\mathcal{W}_c) = f_c^{-1}(\mathcal{W}_c)$. In the corresponding four intervals we set $\rho_1(t) = \eta/2^{8.75}$ and $\rho_2(t) = \eta/2^{8.5}$. The next preimages belong to eight t-intervals. Here we set $\rho_1(t) = \eta/2^{9.5}$, and $\rho_2(t) = \eta/2^{9.25}$. On the sixteen intervals of next order preimages we set $\rho_1(t) = \eta/2^{10.25}$, and $\rho_2(t) = \eta/2^{10}$ is the standard value, so that no more modifications are needed. This is important, since some of the next order preimages belong to the critical edge, where the inner border was already defined to be mapped to $\rho_2(t) = \eta/2^{10}$. The "curves" ∂U_1^c and ∂U_2^c are transfered to $\partial U_i^c = \Phi_c^{-1}(\exp \partial U_i)$. A subset of the smoothed curves is sketched in the left part of Figure 13.

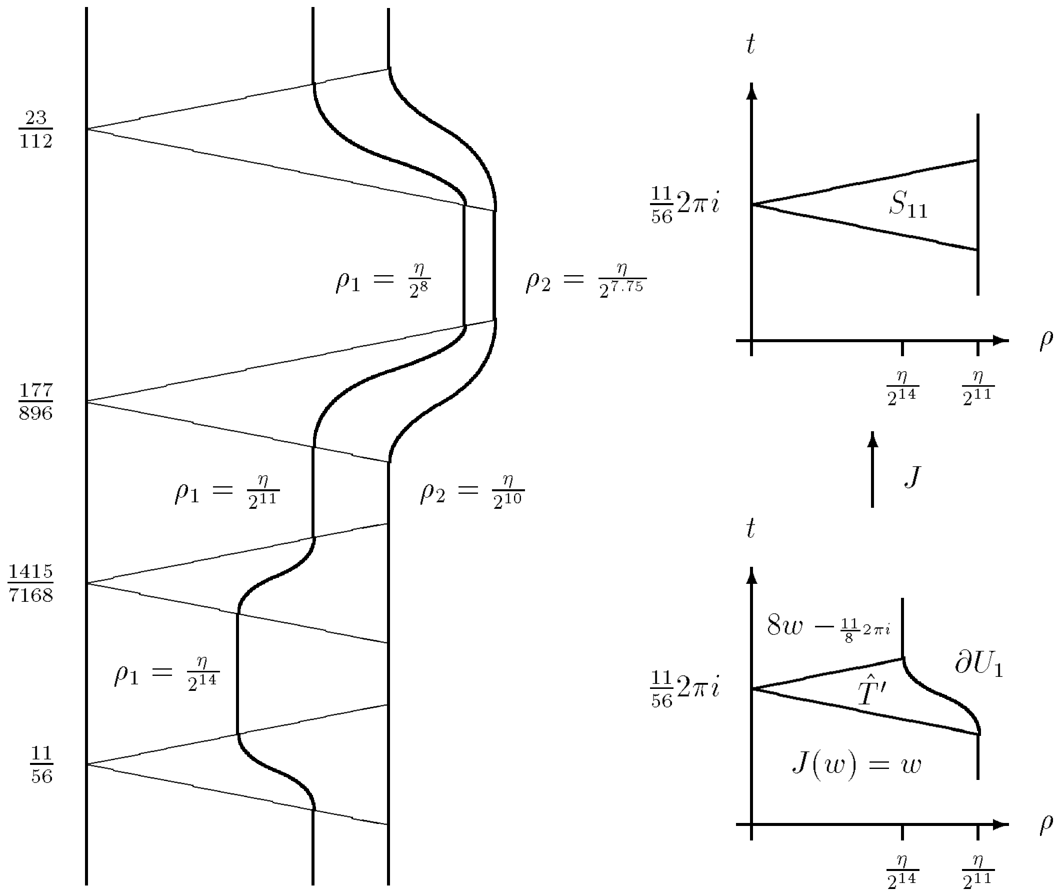

Figure 13: Left: Construction of the boundaries ∂U_i^c. Right: Mapping a sector, cf. Section 13.4.

13.4 Construction of a smooth function g_c

We have fixed the sector parameters s and η with $s\eta < 1/14$ in Section 13.3. Up to now, $j_c^{(1)}$ and $g_c^{(1)}$ have shift discontinuities along eight dynamical rays, and the "curves" ∂U_i^c have a number of step discontinuities. We shall at the same time define j_c as a smooth function in sectors around these rays, and modify ∂U_i^c accordingly. We start with a sector around $\mathcal{R}_c(11/56)$ and define $j_c(z)$ by the conjugate function $J(w)$. Up to now we have $J^{(1)}(w) = w$ and $\rho_1(t) = \eta/2^{11}$ for $t < 11/56$, and $J^{(1)}(w) = 8w - \frac{11}{8}2\pi i$ and $\rho_1(t) = \eta/2^{14}$ for $t > 11/56$. f_c maps $S_{11}^c(11/56)$ onto $S_{10}^c(11/28)$, which touches ∂U_2^c. We require ∂U_1, a "sector" $\hat{T}'(11/56) \subset S_{11}(11/56)$ and $J : \hat{T}'(11/56) \to S_{11}(11/56)$ such that:

- ∂U_1 is a smooth curve, with $\rho_1(t)$ constant below and above the sector, and $\rho_1(t) \le \eta/2^{11}$ within the sector. $\hat{T}'(11/56)$ is bounded by $\partial S_{11}(11/56)$ and ∂U_1 as sketched in the right part of Figure 13.
- J is a homeomorphism $\overline{\hat{T}'(11/56)} \to \overline{S_{11}(11/56)}$, continuously differentiable on $\overline{\hat{T}'(11/56)} \setminus \{\frac{11}{56}2\pi i\}$, and quasi-conformal.

- $J(w)$ is tangent to w on the lower and tangent to $8w - \frac{11}{8}2\pi i$ on the upper border of $\hat{T}'(11/56)$ (thus it cannot be differentiable at the vertex $\frac{11}{56}2\pi i$).

To see that these requirements can be fulfilled, consider

$$J(w) = \frac{11}{56}2\pi i + \Big(w - \frac{11}{56}2\pi i\Big)\, r\Big(\frac{t - \frac{11}{56}}{s\rho}\Big) ,$$

where $r \in C^1([-1, 1], \mathbb{R})$ satisfies $r(-1) = 1$, $r(1) = 8$, $r'(-1) = r'(1) = 0$ and $r(x) \geq 1$ for $-1 \leq x \leq 1$. Define $\partial U_1 = J^{-1}(\partial U_2)$ and $\hat{T}'(11/56)$ accordingly. Then $r(x) \geq 1$ implies $\rho_1(t) \leq \eta/2^{11}$, and $r'(\pm 1) = 0$ makes J tangent to the map defined below and above the sector. Any orientation-preserving diffeomorphism is quasi-conformal on a compact set. This argument cannot be applied directly, since the vertex is excluded from $\overline{\hat{T}'(11/56)}$. But one checks that DJ depends only on the variable $x = \frac{t-\frac{11}{56}}{s\rho}$, thus the Beltrami coefficient of J stays bounded away from 1 as w approaches the vertex $\frac{11}{56}2\pi i$. In [1] and [4] a different construction for J is used: It is defined recursively on a countable family of "rectangles" filling out $\hat{T}'(\theta)$.
Now $j_c : \hat{T}_c'(11/56) \to S_{11}^c(11/56)$ and $g_c = f_c \circ j_c : \hat{T}_c'(11/56) \to S_{10}^c(11/28)$ are quasi-conformal. We employ a similar construction for 1415/7168, 1913/7168 and 15/56. For the other four rays, we construct J and the inner boundary in the same way, and define the outer boundary smoothly. The boundaries at the preimages of these four sectors are defined recursively, the inner boundary is obtained as a preimage under f_c, and the outer boundary can be chosen appropriately. Then U_1^c and U_2^c are bounded, simply connected domains with smooth boundaries and $\overline{U_1^c} \subset U_2^c$. The mapping $g_c : U_1^c \to U_2^c$ is proper of degree 2 and quasi-regular, since $j_c : U_1^c \to f_c^{-1}(U_2^c)$ is quasi-conformal. These mappings are C^1 except at four points, and holomorphic except in eight sectors.
For each of the eight sectors $\hat{T}_c'(\theta)$, define $T_c'(\theta) = S_0^c(\theta) \cap U_2^c$. Define T_c' as the union of these eight sectors, then g_c is holomorphic in $U_1^c \setminus T_c'$, and set $T_c'' = \bigcup\limits_{n=1}^{\infty} g_c^{-n}(T_c')$. The Beltrami coefficient $\frac{\overline{\partial} j_c}{\partial j_c}$ of j_c has an extension to $\mathbb{C}$, which vanishes outside of T_c' and is continuous except at four points.

13.5 Orbits under g_c

The definition (15) of j_c (outside of T_c' we have $j_c = j_c^{(1)}$) implies

$$\begin{aligned}
z \in \mathcal{U}_c \cap U_1^c \setminus T_c' &\Rightarrow g_c^3(z) = f_c^6(z) , \quad g_c^n(z) \notin \mathcal{U}_c \cup \mathcal{V}_c \cup \mathcal{W}_c \text{ for } 1 \leq n \leq 3 \\
z \in \mathcal{V}_c \cap U_1^c \setminus T_c' &\Rightarrow g_c^{10}(z) = f_c^{10}(z) , \quad g_c^n(z) \notin \mathcal{U}_c \cup \mathcal{V}_c \cup \mathcal{W}_c \text{ for } 1 \leq n \leq 9 \\
z \in \mathcal{W}_c \cap U_1^c \setminus T_c' &\Rightarrow g_c^7(z) = f_c^4(z) , \quad g_c^n(z) \notin \mathcal{U}_c \cup \mathcal{V}_c \cup \mathcal{W}_c \text{ for } 1 \leq n \leq 6 .
\end{aligned} \tag{16}$$

Thus the orbit of z under g_c returns to the orbit of z under f_c. If z_0 is p-periodic under f_c, thus $f_c^p(z_0) = z_0$ with p minimal, then z_0 is periodic under g_c with a period q satisfying $\frac{4}{7}p \leq q \leq \frac{7}{4}p$. The images $g_c^n(z_0)$ are periodic or preperiodic under f_c. We have $g_c^q(z) = f_c^p(z)$ for z in a neighborhood of z_0, and $g_c^{q\prime}(z_0) = f_c^{p\prime}(z_0)$. Since the multiplier is the same, the cycle of g_c is attracting, iff the cycle of f_c is.

$g_c : U_1^c \to U_2^c$ is polynomial-like of degree 2, except that it is not holomorphic. If we define $\mathcal{K}_g := \{z \in U_1^c \,|\, g_c^n(z) \in U_1^c \text{ for } n \in \mathbb{N}\}$, then we have $\mathcal{K}_g = \mathcal{K}_c$, since: If $z \in \mathcal{K}_c$ we have $g_c^n(z) \in \mathcal{K}_c$ for $n \in \mathbb{N}$, since $\mathcal{K}_c$ is completely invariant under f_c and $z \mapsto -z$. If $z \in T_c' \cup T_c''$ and $g_c^n(z)$ is defined for sufficiently large n, then $g_c^n(z) \in S_0^c$ for $n \geq n_0$. Now $g_{c|S_0^c} = f_{c|S_0^c}$, thus $g_c^n(z)$ leaves U_1^c after a finite number of iterations. If $z \in U_1^c \setminus (\mathcal{K}_c \cup T_c' \cup T_c'')$, the orbit $g_c^n(z)$ leaves U_1^c, since otherwise there would be sequences n_k, $m_k \to \infty$ $(k \to \infty)$ with $g_c^{n_k}(z) = f_c^{m_k}(z)$, but $f_c^m(z)$ leaves U_1^c for $m \to \infty$.

The "sectors" in $T_c' \cup T_c''$ are contained in sectors of f_c (cf. Section 13.1):

$$\begin{aligned}
&T_c'(11/56) = S_{10}^c(11/56) \subset S_3^c(11/56) \subset S_c \\
&T_c'(1415/7168) = S_{10}^c(1415/7168) \subset S_c \\
&T_c'(177/896) \subset S_8^c(177/896) \subset S_7^c(177/896) \subset S_c \\
&T_c'(23/112) \subset S_8^c(23/112) \subset S_4^c(23/112) \subset S_c \ ,
\end{aligned}$$

and similarly for the four sectors on the other side of the critical edge. The equality for $\theta = 1415/7168$ motivated our choice of $\eta/2^{10}$ for ∂U_2^c. We claim that the sectors in $T_c'' = \bigcup\limits_{n=1}^{\infty} g_c^{-n}(T_c')$ have the following properties: They are contained in sectors of S_c, thus they are disjoint, and no orbit (under g_c) is visiting the same sector twice. This follows from the fact that for any $T_c''(\theta) \subset T_c''$ there are n, m with $g_c^n(T_c''(\theta)) = f_c^m(T_c''(\theta))$. For example, $S_{14}^c(\frac{22919}{114688})$ belongs both to T_c'' and to S_c. It is mapped by g_c^7 and by f_c^4 onto $S_{10}^c(\frac{1415}{7168})$, which belongs both to T_c' and to S_c.

13.6 Obtaining a holomorphic mapping

The sets T_c' and T_c'' have been defined in Section 13.4. We want to define a measurable Beltrami coefficient (or ellipse field) that is invariant under g_c (in the sense of Section 11.2). We set $\mu_c(z) = 0$ for $z \in U_2^c \setminus (T_c' \cup T_c'')$, especially for $z \in \mathcal{K}_c$. For $z \in \hat{T}_c'$ we set $\mu_c(z) = \dfrac{\overline{\partial} g_c(z)}{\partial g_c(z)}$, since $\mu_c = 0$ in $g_c(\hat{T}_c')$. μ_c is extended continuously to $T_c' \setminus \hat{T}_c'$, so that it vanishes on $\partial T_c'$, except at the four vertices. If $z \in T_c''$, there is a unique n with $g_c^n(z) \in T_c'$. $\mu_c(z)$ is defined recursively, such that the ellipse field in $g_c^{-n}(T_c')$ is mapped by $T_z g_c$ onto that defined before in $g_c^{-(n-1)}(T_c')$. $\mu_c(z)$ is bounded by $M < 1$ on T_c' since g_c is quasi-regular, and the same M holds on U_2^c, since g_c is holomorphic in T_c''. Now $\mu_c(z)$ will be discontinuous on $\mathcal{J}_c = \partial\mathcal{K}_c$. But its restrictions to $\mathcal{K}_c$ and to $U_2^c \setminus \mathcal{K}_c$ are continuous, thus $\mu_c(z)$ is measurable. By the Measurable Riemann Mapping Theorem, there is a quasi-conformal mapping $\phi_c : U_2^c \to \mathbb{D}$ with $\dfrac{\overline{\partial}\phi_c}{\partial\phi_c} = \mu_c$, thus sending the infinitesimal ellipse field to circles. Thus $\phi_c \circ g_c \circ \phi_c^{-1} : \phi_c(U_1^c) \to \mathbb{D}$ is holomorphic, since it sends infinitesimal circles to circles. This function is polynomial-like of degree 2, with the filled Julia set $\phi_c(\mathcal{K}_c)$. In the notation of [4], we have $g_c^{(1)} = f_c^{(1)}$, $g_c = f_c^{(2)}$ and $\phi_c \circ g_c \circ \phi_c^{-1} = f_c^{(3)}$.

$$\begin{tikzcd}
\mathbb{C} \arrow[d, "f_c"] & \mathbb{C} \setminus \bigcup_{j=1}^{8} \mathcal{R}_c(\theta_j) \arrow[d, "g_c^{(1)}"] & U_1^c \arrow[r, "\phi_c"] \arrow[d, "g_c"] & \phi_c(U_1^c) \arrow[r, "\chi_c"] \arrow[d, "\phi_c \circ g_c \circ \phi_c^{-1}"] & U_1^{c\prime} \arrow[d, "f_d"] \\
\mathbb{C} & \mathbb{C} \setminus \bigcup_{j=1}^{8} \mathcal{R}_c(\theta'_j) & U_2^c \arrow[r, "\phi_c"] & \mathbb{D} \arrow[r, "\chi_c"] & U_2^{c\prime}
\end{tikzcd}$$

Figure 14: Some mappings of Sections 13.6 and 13.7.

13.7 Definition of h

We apply the Straightening Theorem to the polynomial-like mapping $\phi_c \circ g_c \circ \phi_c^{-1}$ of Section 13.6. There is a hybrid-equivalence χ_c and a unique parameter $d \in \mathcal{M}$ with $\chi_c \circ (\phi_c \circ g_c \circ \phi_c^{-1}) \circ {\chi_c}^{-1} = f_d$ on $U_1^{c\prime}$, where we define $\psi_c = \chi_c \circ \phi_c$ and $U_i^{c\prime} = \psi_c(U_i^c)$. We have $\psi_c(0) = 0$ and $\psi_c(c) = d$. (At first, χ_c is defined in a neighborhood of $\phi_c(\mathcal{K}_c)$, but it can be extended to $\overline{\mathbb{D}}$, cf. [4, Remarks 5.5].)
Since $\mathcal{K}_c$ is invariant under g_c, $\psi_c(\mathcal{K}_c)$ is invariant under f_d, thus $\psi_c(\mathcal{K}_c) \subset \mathcal{K}_d$. The preimages of α_c or β_c under f_c and under g_c are dense in $\mathcal{J}_c$ and those of α_d under f_d are dense in $\mathcal{J}_d$. Thus $\psi_c(\mathcal{J}_c) = \mathcal{J}_d$, and $\psi_c(\mathcal{K}_c) = \mathcal{K}_d$. Now $\mathcal{K}_d \setminus \{\alpha_d\}$ has three connected components that are mapped in the order characteristic of $d \in \mathcal{M}_{1/3}$. Thus $\psi_c(\alpha_c) = \alpha_d$ and $\psi_c(\beta_c) = \beta_d$, and every vertex of $\mathcal{K}_c$ is mapped by ψ_c onto the corresponding vertex of $\mathcal{K}_d$. Especially, the edge from $\gamma_c(11/56)$ to $\gamma_c(23/112)$ is mapped onto the corresponding edge, and $d = \psi_c(c)$ belongs to the edge from $\gamma_d(11/56)$ to $\gamma_d(23/112)$.
Thus by $h(c) := d$ we obtain a mapping of the parameter edge $\mathcal{E}_M$ from $a = \gamma_M(11/56)$ to $b = \gamma_M(23/112)$ into itself. We will define a similar mapping $\tilde{h}$ in Section 13.9, show in Section 14 that h and $\tilde{h}$ are mutually inverse, and prove continuity in Section 15. Thus h is a homeomorphism.

13.8 Independence of the choices

In the construction of h, we have chosen values of s and η, the diffeomorphism j_c in some sectors, smooth parts of the boundary ∂U_2^c, and μ in $U_2^c \setminus U_1^c$. Although these choices can be made uniformly for $c \in \mathcal{E}_M$, it is interesting to note that h is independent of them. Suppose that g_c and U_i^c were constructed with s, η, and $\hat{g}_c$, $\hat{U}_i^c$ were constructed with $\hat{s}$, $\hat{\eta}$. Assume $\psi_c \circ g_c \circ \psi_c^{-1} = f_d$ and $\hat{\psi}_c \circ \hat{g}_c \circ \hat{\psi}_c^{-1} = f_{\hat{d}}$, then we want to show $d = \hat{d}$.
First note that d does not change when η is decreased or s is increased, thus we may assume $s = \hat{s}$ and $\eta = \hat{\eta}$. Then we construct a homeomorphism $\xi : U_2^c \to \hat{U}_2^c$

with $\xi \circ g_c \circ \xi^{-1} = \hat{g}_c$ on $\hat{U}_1^c$. The idea is to define it recursively in the sectors, and ξ is the identity outside of the sectors (here we need $s = \hat{s}$, thus the sectors are equal). ξ is quasi-conformal with $\overline{\partial}\xi = 0$ almost everywhere on $\mathcal{K}_c$, thus f_d and $f_{\hat{d}}$ are hybrid-equivalent, and $d = \hat{d}$.

13.9 The inverse mapping

The mapping $\tilde{h} : \mathcal{E}_M \to \mathcal{E}_M$ is constructed step by step in the same way as h, by taking

$$\tilde{j}_c^{(1)}(z) = \begin{cases} f_c^{-6} \circ f_c^3 & , \quad z \in \mathcal{U}_c' \\ f_c^{-9} \circ (-f_c^9) & , \quad z \in \mathcal{V}_c' \\ f_c^{-3} \circ (-f_c^6) & , \quad z \in \mathcal{W}_c' \\ z & , \quad \text{otherwise}, \end{cases} \tag{17}$$

instead of $j_c^{(1)}$. Then we form $\tilde{g}_c^{(1)} = f_c \circ \tilde{j}_c^{(1)}$, and $\tilde{\psi}_c \circ \tilde{g}_c \circ \tilde{\psi}_c^{-1} = f_d$ defines $\tilde{h}(c) = d$. We will show in Section 14 that h and $\tilde{h}$ are mutually inverse.

14 Proof that h is Bijective

The following Lemma and its proof are analogous to Theorem G in [4].

Lemma 11 *In Section 13 we constructed a quasi-conformal homeomorphism ψ_c with $\psi_c \circ g_c \circ \psi_c^{-1} = f_d$ for $d = h(c)$, and $\overline{\partial}\psi_c = 0$ a.e. on $\mathcal{K}_c$. g_c was defined by making some choices, especially of $s\eta < 1/14$. Assume $\tilde{s}\tilde{\eta} < 1/14$. Then there is a mapping Ψ_c with the same properties as ψ_c given above and*

- *Ψ_c maps U_2^c onto the interior of the Green's line $G_d(z) = \tilde{\eta}$.*
- *The sectors of slope s around the eight external rays $\mathcal{R}_c(\theta_j)$ defining $\mathcal{U}_c$, $\mathcal{V}_c$, $\mathcal{W}_c$ are mapped onto the sectors of slope $\tilde{s}$ around the eight external rays $\mathcal{R}_d(\theta_j')$ defining $\mathcal{U}_d'$, $\mathcal{V}_d'$, $\mathcal{W}_d'$.*

Assume that c, d, $e \in \mathcal{E}_M$ with $d = h(c)$ and $e = \tilde{h}(d)$. We want to show $e = c$, thus $\tilde{h} \circ h = \mathrm{id}_{\mathcal{E}_M}$, and $h \circ \tilde{h} = \mathrm{id}_{\mathcal{E}_M}$ is analogous. Choose Ψ_c according to Lemma 11 with $\Psi_c \circ g_c \circ \Psi_c^{-1} = f_d$. Now g_c equals $g_c^{(1)} = f_c \circ j_c^{(1)}$ in $U_1^c \setminus T_c'$, where $j_c^{(1)}$ is given by (15) on page 34. $\tilde{g}_d$ equals $\tilde{g}_d^{(1)} = f_d \circ \tilde{j}_d^{(1)}$ given by (17) in $\tilde{U}_1^d \setminus \tilde{T}_d'$. In most parts of $\tilde{U}_1^d$ we have

$$\tilde{g}_d = f_d = \Psi_c \circ g_c \circ \Psi_c^{-1} = \Psi_c \circ f_c \circ \Psi_c^{-1} \ .$$

In $\tilde{U}_1^d \cap \mathcal{U}_d' \setminus \tilde{T}_d'$ we have

$$\tilde{g}_d = f_d^{-5} \circ f_d^3 = (\Psi_c \circ g_c \circ \Psi_c^{-1})^{-5} \circ (\Psi_c \circ g_c \circ \Psi_c^{-1})^3 = \Psi_c \circ (g_c^{-5} \circ g_c^3) \circ \Psi_c^{-1} \ .$$

Here the property $\tilde{T}_d' = \Psi_c(T_c')$ is used. By following the orbit and employing (15) we see

$$g_c^{-5} \circ g_c^3 = g_c^{-5} \circ g_c^2 \circ g_c = f_c^{-5} \circ f_c^2 \circ (f_c^{-2} \circ f_c^6) = f_c \ .$$

The regions $\mathcal{V}_d'$ and $\mathcal{W}_d'$ are treated analogously. Note that $\Psi_c(z^2+c) = (\Psi_c(z))^2 + d$ for z in the puzzle-piece 01 implies $\Psi_c(-z) = -\Psi_c(z)$. We obtain $\tilde{g}_d = \Psi_c \circ f_c \circ \Psi_c^{-1}$ in $\tilde{U}_1^d \setminus \tilde{T}_d'$. Proceeding as in Section 13.8, we see that $\tilde{g}_d$ and f_e are hybrid-equivalent to f_c, and thus $e = c$.

Remark: One may show that ψ_c is uniquely determined on $\mathcal{K}_c$, and $\tilde{\psi}_d$ is uniquely determined on $\mathcal{K}_d$, cf. Proposition 5.6 in [4]. Thus ψ_c and $\tilde{\psi}_d$ are mutually inverse on the filled-in Julia set.

15 Proof that h is Continuous

Our $g_c(z)$ and $\mu_c(z)$ does not depend holomorphically on c for fixed z. We do not expect $\phi_c \circ g_c \circ \phi_c^{-1}$ to depend analytically on the parameter c, thus the result of [8, p.313] on continuity of $h(c)$ cannot be applied.

We prove continuity of h by distinguishing between three cases below. The Closed Graph Theorem says that the following statements are equivalent, since $h : \mathcal{E}_M \to \mathcal{E}_M$ is bijective and $\mathcal{E}_M$ is compact:

1. h is continuous.
2. $\tilde{h} = h^{-1}$ is continuous.
3. If $c_n \to c$ and $d_n := h(c_n) \to \tilde{d}$, then $\tilde{d} = h(c)$.

Thus we do not have to consider $\tilde{h}$ separately, and 3. means that we can pass to a subsequence of $\{c_n\}$.

15.1 Analyticity of h in hyperbolic components

Recall the remarks on (16). Suppose that Ω is a hyperbolic component of period p in $\mathcal{E}_M$ and $\lambda = \rho(c)$ is the corresponding multiplier map. For every $c \in \Omega$, the critical orbit of g_c is qualitatively the same, since we can perform the surgery on the Hubbard tree. Thus all $d = h(c)$ belong to the same hyperbolic component $\tilde{\Omega}$ of period $\frac{4}{7}p \le q \le \frac{7}{4}p$, and we have seen that the multipliers are the same. With $\tilde{\rho} : \tilde{\Omega} \to \mathbb{D}$ we obtain the representation $h = \tilde{\rho}^{-1} \circ \rho$ on Ω.

15.2 Analyticity of h in non-hyperbolic components

c belongs to a non-hyperbolic component of $\mathring{\mathcal{M}}$ (which are conjectured not to exist at all), iff $\mathcal{J}_c$ has positive measure and carries an invariant line field. This yields a parameterization of the component by the unit disk, and this mapping is compatible with h. See the proof of the corresponding result and the references in [4, Section 5.4].

15.3 Continuity of h at the boundary

Assume that $c \in \partial\mathcal{E}_M = \mathcal{E}_M \cap \partial\mathcal{M}$ and $c_n \in \mathcal{E}_M$ with $c_n \to c$. Set $d_n = h(c_n)$ and $d = h(c)$. Since h maps $\overset{\circ}{\mathcal{E}}_M \to \overset{\circ}{\mathcal{E}}_M$, we have $d \in \partial\mathcal{E}_M$. By the Closed Graph Theorem we may assume that $d_n \to \tilde{d} \in \mathcal{E}_M$, and we must show $\tilde{d} = d$. We have

$$\begin{aligned} f_{d_n} &= \psi_{c_n} \circ g_{c_n} \circ \psi_{c_n}^{-1} &&= \chi_{c_n} \circ (\phi_{c_n} \circ g_{c_n} \circ \phi_{c_n}^{-1}) \circ \chi_{c_n}^{-1} \\ f_d &= \psi_c \circ g_c \circ \psi_c^{-1} &&= \chi_c \circ (\phi_c \circ g_c \circ \phi_c^{-1}) \circ \chi_c^{-1} \ . \end{aligned}$$

We assume that $U_2^{c_n}$, U_2^c and j_{c_n}, j_c have been defined in the same way in the w-halfstrip, and pulled back by $\Phi_c^{-1} \circ \exp$ to the z-plane. Then $\partial U_2^{\hat{c}}$ can be defined for $\hat{c}$ in a neighborhood of c, and the ϕ_{c_n} are (uniformly) K-quasi-conformal.

Lemma 12 *There is a subsequence $\{c_n'\}$ and a quasi-conformal mapping $\phi_* : U_2^c \to \mathbb{D}$ with $\phi_{c_n'} \circ g_{c_n'} \circ \phi_{c_n'}^{-1} \to \phi_* \circ g_c \circ \phi_*^{-1}$ uniformly on compact subsets of $\phi_*(U_1^c) \subset \mathbb{D}$.*

By the same arguments as in [4, Section 5.5], we obtain a subsequence $\{c_n''\}$ with $\chi_{c_n''} \to \chi_*$, and finally

$$f_{d_n''} \to \chi_* \circ (\phi_* \circ g_c \circ \phi_*^{-1}) \circ \chi_*^{-1} = (\chi_* \circ \phi_* \circ \phi_c^{-1} \circ \chi_c^{-1}) \circ f_d \circ (\chi_* \circ \phi_* \circ \phi_c^{-1} \circ \chi_c^{-1})^{-1} \ .$$

On the other hand, $d_n \to \tilde{d}$ implies $f_{d_n''} \to f_{\tilde{d}}$. Thus $f_d \overset{\text{qc}}{\sim} f_{\tilde{d}}$, and $d \in \partial\mathcal{M}$ implies $d = \tilde{d}$. This ends the proof of continuity at $c \in \partial\mathcal{E}_M$. ∎

Proof of Lemma 12 (see [4, Section 5.5] for details and references):
The extended λ-Lemma for holomorphic motions yields a sequence of K'-quasi-conformal mappings $H_{c_n} : U_2^c \to U_2^{c_n}$ with $H_{c_n} \to \mathrm{id}_{U_2^c}$. Consider

$$\phi_{c_n} \circ g_{c_n} \circ \phi_{c_n}^{-1} = (\phi_{c_n} \circ H_{c_n}) \circ (H_{c_n}^{-1} \circ g_{c_n} \circ H_{c_n}) \circ (\phi_{c_n} \circ H_{c_n})^{-1} \ .$$

$g_{\hat{c}}(z)$ depends continuously on $\hat{c}$, thus $H_{c_n}^{-1} \circ g_{c_n} \circ H_{c_n} \to g_c$. The convergence theorem of Section 11.1 yields a subsequence $\phi_{c_n'} \circ H_{c_n'} \to \phi_*$. ∎

16 The Mapping of External Arguments

The polynomial $f_c(z) = z^2 + c$ induces the mapping F of external arguments $\theta \in S^1 = \mathbb{R}/\mathbb{Z}$ given by $F(\theta) = 2\,\theta\,(\mathrm{mod}\,1)$. Now g_c and $\tilde{g}_c$ induce $G, \tilde{G} : S^1 \to S^1$ with

$$G(\theta) = \begin{cases} 16\,\theta - 11/4 & , \ 11/56 \le \theta \le 1415/7168 \\ 2\,\theta + 7/512 & , \ 1415/7168 \le \theta \le 177/896 \\ \theta/4 + 23/64 & , \ 177/896 \le \theta \le 23/112 \\ \theta/4 + 29/64 & , \ 29/112 \le \theta \le 239/896 \\ 2\,\theta - 7/512 & , \ 239/896 \le \theta \le 1913/7168 \\ 16\,\theta - 15/4 & , \ 1913/7168 \le \theta \le 15/56 \\ 2\,\theta & , \ \text{otherwise,} \end{cases} \tag{18}$$

$$\tilde{G}(\theta) \;=\; \begin{cases} \theta/4 + 11/32 & , \quad 11/56 \le \theta \le 183/896 \\ 2\,\theta - 7/512 & , \quad 183/896 \le \theta \le 1465/7168 \\ 16\,\theta - 23/8 & , \quad 1465/7168 \le \theta \le 23/112 \\ 16\,\theta - 29/8 & , \quad 29/112 \le \theta \le 1863/7168 \\ 2\,\theta + 7/512 & , \quad 1863/7168 \le \theta \le 233/896 \\ \theta/4 + 15/32 & , \quad 233/896 \le \theta \le 15/56 \\ 2\,\theta & , \quad \text{otherwise} \end{cases} \tag{19}$$

in the following sense: The ray $\mathcal{R}_c(\theta)$ in the dynamical plane of $f_c(z)$ is mapped by g_c onto the ray $\mathcal{R}_c(G(\theta))$. This is true in a strict sense for the preliminary definition of $g_c^{(1)}$ in Section 13.2. For the smoothed g_c of Section 13.4, we consider the "end" of $\mathcal{R}_c(\theta)$ in U_1^c, avoiding $g_c^{-1}(T_c')$. The mappings $\tilde{g}_c$ and $\tilde{G}$ are related in the same way. Now F, G and $\tilde{G}$ are orientation-preserving covering maps of degree 2, and we shall construct conjugating functions H and $\tilde{H}$, which are induced by the homeomorphisms in the dynamical- and the parameter plane, and which can be used to calculate $h(c)$ for $c = \gamma_M(\theta)$, $\theta \in \mathbb{Q}$.

Theorem 13 *The maps F, G, $\tilde{G}$: $S^1 \to S^1$ are covering maps of degree 2, fixing $\theta = 0$.*

1. *There are unique orientation-preserving homeomorphisms H and $\tilde{H}$, fixing 0 and conjugating $H \circ G \circ H^{-1} = F$ and $\tilde{H} \circ \tilde{G} \circ \tilde{H}^{-1} = F$. We have $\tilde{H} = H^{-1}$.*

2. *$H(\theta)$ can be calculated from the orbit of 0 under G (see the explanation and the example below), and $\tilde{H}$ is analogous.*

3. *Suppose that $d = h(c)$, thus $\psi_c \circ g_c \circ \psi_c^{-1} = f_d$. For $\theta \in \mathbb{Q}$ and $z = \gamma_c(\theta) \in \mathcal{K}_c$ we have $\psi_c(z) = \gamma_d(H(\theta)) \in \mathcal{K}_d$, and analogously $\tilde{\psi}_d(\gamma_d(\theta)) = \gamma_c(\tilde{H}(\theta))$. Thus H is induced by ψ_c but independent of c.*

4. *Suppose that $d = h(c)$ and $c = \gamma_M(\theta)$ for a rational $\theta \in [11/56,\, 23/112] \cup [29/112,\, 15/56]$. Then $d = \gamma_M(H(\theta))$, and analogously for $\tilde{h}$ and $\tilde{H}$.*

5. *If $\mathcal{M}$ is locally connected, the homeomorphism h will have a continuous, orientation-preserving extension to $\mathbb{C}$.*

Proof:

1. H is defined recursively on the preimages of 0: Both for F and G, there is one preimage of order 1, two of order 2, four of order 3 ..., and there is exactly one preimage of order n between two consecutive preimages of order $0 \le m \le n-1$. Thus H is uniquely defined on these preimages. The dense set $\mathcal{P} = \{\frac{q}{2^r} \mid q \in \mathbb{N}_0,\, r \in \mathbb{N}_0\}$ is completely invariant both under F and G, thus it contains precisely the preimages of 0. Since $H : \mathcal{P} \to \mathcal{P}$ is monotonous and $\mathcal{P}$ is dense, H has a unique continuous extension to $[0,\, 1]$ by the topological Lemma 7.6 in [4]. See the proof of 4. for $\tilde{H} = H^{-1}$.

2. We have $H \circ G^n(\theta) = F^n \circ H(\theta)$. Thus the n-th digit of the binary expansion of $H(\theta)$ is 0 or 1, according to whether $G^n(\theta)$ is in $[0,\, 1/2)$ or $[1/2,\, 1)$, respectively.

(Note that $H(1/2) = 1/2$.) For $\theta \in \mathbb{R} \setminus \mathbb{Q}$, $H(\theta)$ can be determined to arbitrary precision, and for $\theta \in \mathbb{Q}$, $H(\theta)$ is determined exactly.

3. Assume $z = \gamma_c(\theta)$, $\theta \in \mathbb{Q}$, and set $z' = \psi_c(z) \in \mathcal{K}_d$, $\theta' = H(\theta)$. z' is (pre-)periodic under f_d, since z is (pre-)periodic under g_c by the relations (16). G has similar properties, thus θ' is (pre-)periodic and $\mathcal{R}_d(\theta')$ is landing at $\partial\mathcal{K}_d$. Now z' has the same number of accesses as z has in $\mathcal{K}_c$, and there is a unique θ'', such that $\mathcal{R}_d(\theta'')$ is landing at z' through the same access as $\psi_c(\mathcal{R}_c(\theta))$. The digits of θ'' are determined from the dynamics of z' under f_d, and the digits of θ' are determined from the dynamics of z under g_c. Since these are conjugate, we have $\theta'' = \theta'$.

4. At least for $\theta \in \mathbb{Q}$ we have $c = \gamma_M(\theta) \Leftrightarrow c = \gamma_c(\theta)$, thus the result 3. in the dynamical plane implies the statement in the parameter plane. Now we turn to the remaining claim of 1.:

We do not know how to prove $\tilde{H} = H^{-1}$ from $G = F \circ J$ and $\tilde{G} = F \circ J^{-1}$, since the equations $H \circ F \circ J \circ H^{-1} = F$ and $H^{-1} \circ F \circ J^{-1} \circ H = F$ are not equivalent. But $\tilde{h} = h^{-1}$ implies $\tilde{H} = H^{-1}$ on $E := [11/56,\, 23/112] \cup [29/112,\, 15/56]$. By taking preimages w.r.t. $F = G = \tilde{G}$ restricted to $S^1 \setminus E$, we get $\tilde{H} = H^{-1}$ on a dense set.

An alternative proof employs 3. and the remark on page 41.

5. In the strip (para-puzzle-piece) 1200120, h is continued by mapping $\mathcal{R}_M(\theta) \to \mathcal{R}_M(H(\theta))$ equipotentially. This definition matches continuously with h on $\mathcal{E}_M$, since $\mathcal{R}_M(\theta)$ lands at $\partial\mathcal{M}$ and the landing point depends continuously on θ, if $\mathcal{M}$ is locally connected. h can be the identity outside of the strip. ■

Remarks:

It would be almost impossible to compute $d = h(c)$ numerically from the surgical procedure. But for $c = \gamma_M(\theta)$, $\theta \in \mathbb{Q}$, we can determine $H(\theta)$ combinatorially (in many cases, d can then be computed with the spider algorithm [13] or with the author's mandel.exe). Either perform the surgery on the Hubbard tree of f_c and read off the digits of $H(\theta)$, or consider the orbit of θ under G (this is implemented in mandel.exe). Example:

$$\frac{25}{127} \overset{G}{\mapsto} \frac{203}{4\cdot 127} \overset{G}{\mapsto} \frac{203}{2\cdot 127} \overset{G}{\mapsto} \frac{76}{127} \overset{G}{\mapsto} \frac{25}{127}\,,$$

and we read off the digits $.\overline{0011} = 3/15 = H(25/127)$ from $G^n(\theta) \in [0,\, 1/2)$ or $[1/2,\, 1)$. Note that $\frac{203}{4\cdot 127}$ is preperiodic under F, but $H(\frac{203}{4\cdot 127}) = \frac{6}{15}$ is periodic. For $\theta \in [11/56,\, 23/112] \cup [29/112,\, 15/56]$, the remarks on (16) show that $H(\theta)$ is periodic, iff θ is periodic.

In [4, Chapter 7], Branner and Fagella have proved similar results for their homeomorphisms. They consider not only $\theta \in \mathbb{Q}$ but all rays that land. The mapping H could also be obtained from their Lemma 7.1 (G is expanding in the weak sense that for every θ, some iterate G^n is strictly expanding around θ): Take $H_0(\theta) = \theta$ and define H_n recursively by $F \circ H_n = H_{n-1} \circ G$, then $H_n \to H$.

In [11], Fagella announces that $\Phi^q_{pp'}$ can be extended without the assumption that $\mathcal{M}$ is locally connected. She conjectures that the (extended?) homeomorphism in the parameter plane is quasi-conformal. Our h will be K-quasi-conformal outside of $\mathcal{M}$, iff H is weakly differentiable with $1/K \le H'(\theta) \le K$. Consider the angles $\alpha_n = \frac{2^{n-1}-1}{2^n-1}$, $\alpha_\infty = 1/2 = .0\overline{1}$, and θ_n, θ_∞ shall be obtained by tuning with $\gamma_M(25/127)$. Their images under H are obtained by tuning with $\gamma_M(3/15)$. Now we have $\theta_\infty - \theta_n \sim k_1\, 2^{-7n}$ and $H(\theta_\infty) - H(\theta_n) \sim k_2\, 2^{-4n}$, thus H is Hölder continuous at θ_∞ with exponent $4/7$, but not Lipschitz continuous. H cannot have a bounded derivative, and our extended homeomorphism h will not be quasi-conformal, but there might be a different extension, which maps the rays not equipotentially, and which is quasi-conformal.

17 Generalization

The preceding sections concentrated on the homeomorphisms h, $\tilde{h}$ of the edge $\mathcal{E}_M$ from a to b. We are not going into details now, but the following generalizations shall be straightforward:

- Analogous homeomorphisms can be defined on every edge of $\mathcal{M}_{1/3}$, except for the trunk. The construction is the same in the following sense: A mapping $\hat{\jmath}_c$ can be defined in the same way for all c in the left branch, so that it provides a shift on the edge from α_c to $-\alpha_c$. If an edge $\mathcal{E}_c^{(m)}$ of $\mathcal{K}_c$ is mapped onto that edge by f_c^m, we construct a homeomorphism of the corresponding parameter edge $\mathcal{E}_M^{(m)}$ by setting $j_c = f_c^{-m} \circ \hat{\jmath}_c \circ f_c^m$ on $\mathcal{E}_c^{(m)}$ for $c \in \mathcal{E}_M^{(m)}$, and $g_c = f_c \circ j_c$. (One might expect that $g_c = f_c \circ \hat{\jmath}_c$ would yield a homeomorphism for all edges at once, but this construction is quite pathological.)

- If v is a vertex of order $n \ge 4$, thus $f_v^n(v) = \alpha_v$, we construct a homeomorphism h_v piecewise, that is expanding around v on the three incident edges. It has the same behavior as F_v^3 with $F_v = f_v^{-n} \circ f_v \circ f_v^n$ around $v \in \mathcal{K}_v$. Now h_v can be considered as a dynamic on $\mathcal{M}$, that is "conjugate" to F_v^3 around v by Tan Lei's similarity. There is no homeomorphism similar to F_v in the parameter plane, since the frames on different edges at v have a different orientation.

- We can obtain further homeomorphisms on the edges, which map the frames in a different way. The simplest example is a homeomorphism h' on the edge $\mathcal{E}_M$ from a to b, which maps $\mathcal{F}_7^M(25,\, 34)$ onto $\mathcal{F}_{10}^M(202,\, 273)$. Such homeomorphisms are obtained from $\hat{\jmath}_c$, if a subset of $\mathcal{E}_M$ is mapped onto the edge from α_c to $-\alpha_c$ by some iterate of f_c. By compositions of h and h', we prove that all frames on the same edge are homeomorphic, which is a stronger statement than Theorem 10.

- A frame contains hierarchies of "secondary frames" (see Section 9.2), e.g. on the arc from $\gamma_M(179/896)$ to $\gamma_M(2865/14336)$. These are homeomorphic to each other by a construction involving $\hat{\jmath}_c$ as above. Presumably this remains true when an arc contains a family that is not a true hierarchy. The procedure can be continued: Each secondary frame contains hierarchies of homeomorphic "tertiary" frames ... .

- The parameter frames are defined on the upper branches of every limb of $\mathcal{M}$, cf. Section 10, and there exist similar homeomorphisms. These will be compatible with the Branner–Douady homeomorphism Φ_A [1] and with the Branner–Fagella homeomorphisms $\Phi^q_{pp'}$ [4].

The combinatorial and topological surgery is easier than the technical details of the holomorphic surgery and of showing that the mapping is a homeomorphism. It would be nice to have a general theorem which says that it is sufficient to work out the topological part. Such a theorem may be feasible in our case, but it will be much harder if higher degree polynomials and Riemann surfaces are involved. In [11], Fagella lists such a general theorem as an open problem.
Our work suggests the following questions:

- Is the exceptional set "between" the parameter frames a Cantor set?
- Is there a reasonable homeomorphism on the trunk of $\mathcal{M}_{1/3}$?
- Let us say that the frames in Figure 7 on page 20 are $\mathcal{F}_4^M(3,4)$, $\mathcal{F}_5^M(7,8)$ and $\mathcal{F}_6^M(13,14)$. Presumably, $\mathcal{F}_4^M(3,4)$ and $\mathcal{F}_6^M(13,14)$ are not homeomorphic, but $\mathcal{F}_4^M(3,4)$ and $\mathcal{F}_5^M(7,8)$ might be homeomorphic, such that 819/4096 in $\mathcal{F}_4^M(3,4)$ corresponds to ρ_2 in $\mathcal{F}_5^M(7,8)$. Or the first frame might be homeomorphic to a subset of the second one, such that η_1 of $\mathcal{F}_4^M(3,4)$ corresponds to ρ_2 of $\mathcal{F}_5^M(7,8)$.
- Consider again the hierarchy of homeomorphic secondary frames on the arc from $\gamma_M(179/896)$ to $\gamma_M(2865/14336)$. Are these homeomorphic to $\mathcal{F}_4^M(3,4)$? Or to $\mathcal{F}_5^M(7,8)$?
- Are the arms of $\mathcal{F}_4^M(3,4)$ in $177/896 \le \arg_M(c) \le 179/896$ and $233/896 \le \arg_M(c) \le 235/896$ homeomorphic?
- Are they homeomorphic to the arm in $23/112 \le \arg_M(c) \le 25/112$?
- Are the two subsets of $\mathcal{E}_M$ between a and $\gamma_M(177/896)$ and between $\gamma_M(183/896)$ and b homeomorphic?
- If $c_t = \gamma_M(k/2^j)$ is a tip of $\mathcal{M}$, and c is obtained from tuning c_t by c_4, some arm is attached to c. Are these arms homeomorphic?
- Can the secondary limbs of $\mathcal{M}$ be described within a similar *frame*work? If two homeomorphic frames are tuned by the same center, say -1, are their images contained in homeomorphic "frames"? What about the arc from $\gamma_M(17/48)$ to $\gamma_M(3/8)$?

References

[1] B. Branner, A. Douady, Surgery on complex polynomials, in: *Holomorphic dynamics*, Proc. 2nd Int. Colloq. Dyn. Syst., Mexico City, Lect. Notes Math. **1345**, 11–72 (1988).

[2] B. Branner, The Mandelbrot Set, in: *Chaos and Fractals*, R. L. Devaney, L. Keen eds., Proc. symp. appl. math. **39**, AMS 1989.

[3] B. Branner, Puzzles and Para-Puzzles of Quadratic and Cubic Polynomials, in: *Complex Dynamical Systems: The Mathematics behind the Mandelbrot and Julia Sets*, R. L. Devaney ed., Proc. symp. appl. math. **49**, AMS 1994.

[4] B. Branner, N. Fagella, Homeomorphisms between limbs of the Mandelbrot set, preprint (1996). To appear in Journal of Geometric Analysis (1998).

[5] L. Carleson, T. W. Gamelin, *Complex dynamics*, New York, Springer (1993).

[6] R. L. Devaney, The Complex Dynamics of Quadratic Polynomials, in: *Complex Dynamical Systems: The Mathematics behind the Mandelbrot and Julia Sets*, R. L. Devaney ed., Proc. symp. appl. math. **49**, AMS 1994.

[7] A. Douady, Algorithms for computing angles in the Mandelbrot set, in: *Chaotic dynamics and fractals*, Proc. Conf., Notes Rep. Math. Sci. Eng. **2**, 155–168 (1986).

[8] A. Douady, J. H. Hubbard, On the dynamics of polynomial-like mappings, Ann. Sci. École Norm. Sup. **18**, 287–343 (1985).

[9] A. Douady, Chirurgie sur les applications holomorphes, in: *Proc. Int. Congr. Math.*, Berkeley / Calif. 1986, Vol. 1, 724–738 (1987).

[10] J.-P. Eckmann, H. Epstein, Scaling of Mandelbrot sets generated by critical point preperiodicity, Commun. Math. Phys. **101**, 283–289 (1985).

[11] N. Fagella, Surgery on the limbs of the Mandelbrot set, in: *Progress in Holomorphic Dynamics*, H. Kriete ed., Pitman research notes **387**, 139–158.

[12] J. H. Hubbard, Local connectivity of Julia sets and bifurcation loci: Three theorems of J.-C. Yoccoz, in: L. R. Goldberg, (ed.) et al.: *Topological methods in modern mathematics*. Proceedings of a symposium in honor of John Milnor's sixtieth birthday. Houston, TX: Publish or Perish, 467–511, 375–378 (1993).

[13] J. H. Hubbard, D. Schleicher, The Spider Algorithm, in: *Complex Dynamical Systems: The Mathematics behind the Mandelbrot and Julia Sets*, R. L. Devaney ed., Proc. symp. appl. math. **49**, AMS 1994.

[14] W. Jung, Some Curves Forming Cobwebs around Mandelbrot and Julia Sets, preprint in preparation (1999).

[15] J. Milnor, Self-similarity and hairiness in the Mandelbrot set, in: *Computers in Geometry and Topology*, M. C. Tangora ed., Lecture Notes in Pure and Applied Mathematics, Marcel Dekker 1989.

[16] J. Milnor, Local Connectivity of Julia Sets: Expository Lectures, IMS-Preprint 92-11 (1992).

[17] D. Schleicher, Rational External Rays of the Mandelbrot Set, IMS-Preprint 97-13 (1997).

[18] D. Schleicher, On Fibers and Renormalization of Julia Sets and Multibrot Sets, preprint (1998).

[19] Tan Lei, Similarity between the Mandelbrot set and Julia sets, Commun. Math. Phys. **134**, 587–617 (1990).

[20] J. Väisälä, Lectures on n-Dimensional Quasiconformal Mappings, Springer LNM **229**, 1971.

Appendix

Most images show the parameter plane on the left and the dynamical plane on the right.

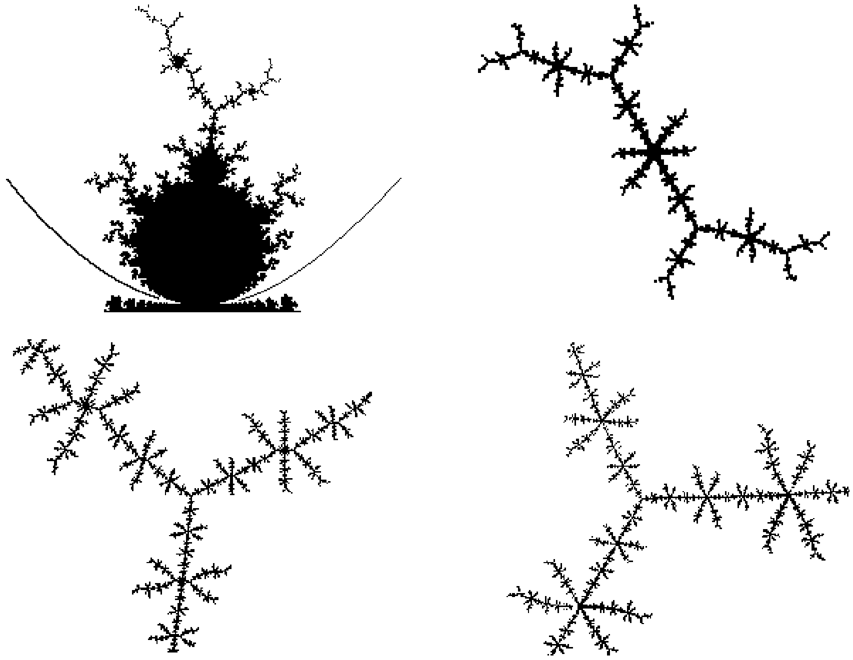

The image above shows magnifications around $a \in \mathcal{M}_{1/3}$ and $a \in \mathcal{K}_a$.
The image below shows the frames $\mathcal{F}_4^M(3, 4)$ and $\mathcal{F}_5^M(5, 6)$ together with the corresponding dynamical frames in $\mathcal{K}_a$. The external rays are $\mathcal{R}_*(\theta_i)$ and $\mathcal{R}_*(\theta'_i)$.

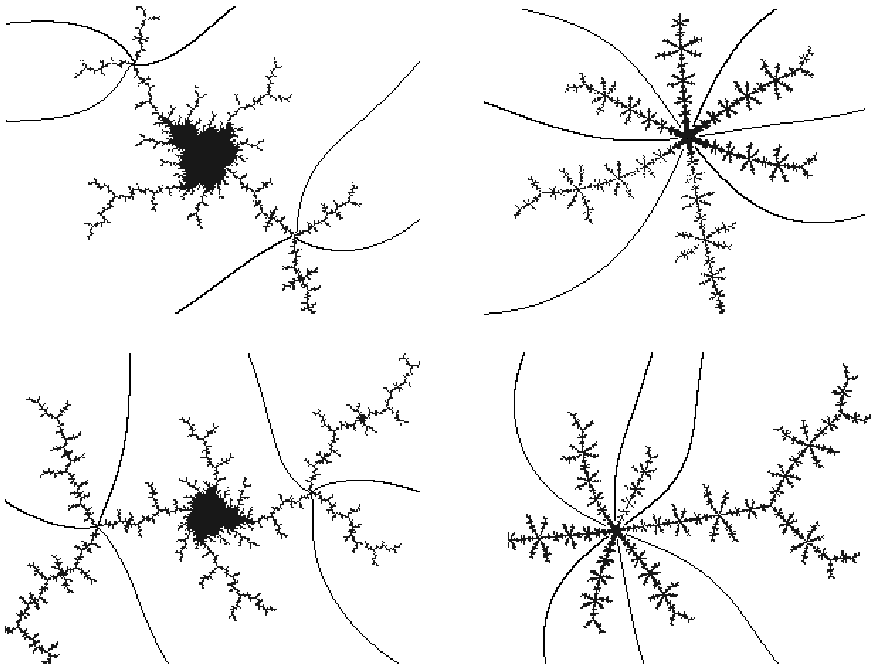

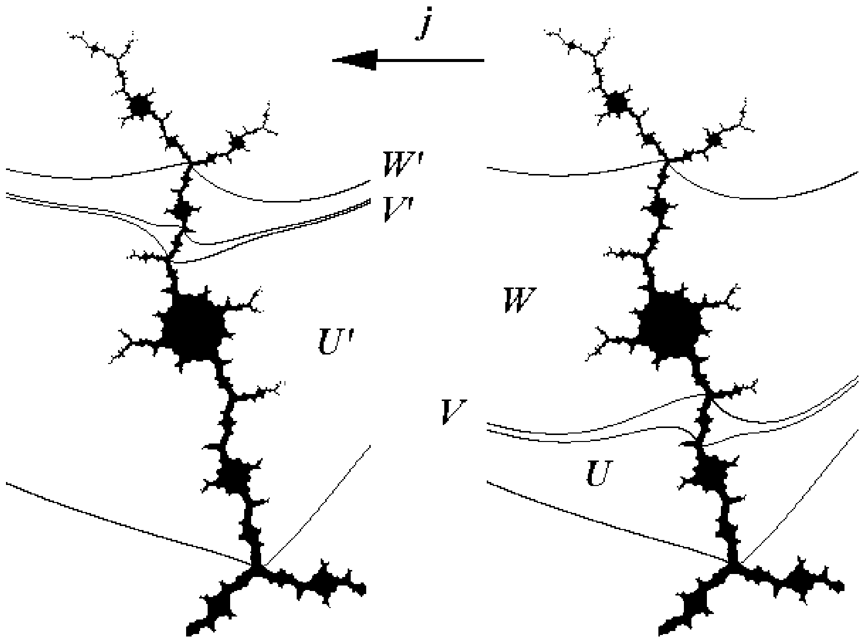

The image above shows the subsets of the critical edge (for c_4) that are important for the construction of g_c, cf. Figure 12 on page 35.
The image below shows the homeomorphic frames $\mathcal{F}_4^M(3,\,4)$ and $\mathcal{F}_7^M(25,\,34)$, together with the homeomorphic Julia sets of the centers c_4 and c_7.